



Article

<https://doi.org/10.1038/s41591-025-04067-x>

Soluble MAdCAM-1 as a biomarker in metastatic renal cell carcinoma

Received: 19 April 2025

Accepted: 16 October 2025

Published online: 07 January 2026

Check for updates

Carolina Alves Costa Silva^{1,2,3,26}, Marc Machaalani^{4,26}, Renee Maria Saliby^{4,5,26}, Caiwei Zhong⁴, Wanling Xie⁴, Edoardo Pasolli^{1,6,7}, Gianmarco Piccinno^{1,8}, Cécile Dalban⁹, Marine Fidelle^{1,10}, Aurelia Meurisse^{11,12}, Dewi Vernerey^{11,12}, Gwo-Shu Mary Lee⁴, Roxanne Birebent^{1,10}, Eddy Saad⁴, Clara Steiner^{1,13}, Ronan Flippot^{14,15,16,17,18}, Janice Barros-Monteiro¹⁹, Nicola Segata^{1,8}, Antoine Thiery-Vuillemin²⁰, Silvia Formenti^{1,21,22,23}, Tatiana Kuznetsova²⁴, Bernard Escudier¹⁵, Lisa Derosa^{1,10,14,15}, Laurence Zitvogel^{1,10,14,15,27}✉, Toni K. Choueiri^{1,25,27} & Laurence Albiges^{1,14,15,27}✉

Patients with metastatic renal cell carcinoma treated with immune checkpoint inhibitors or antiangiogenic tyrosine kinase inhibitors may develop resistance driven by gut dysbiosis, which disrupts the MAdCAM-1- α 4 β 7 axis and promotes the recruitment of immunosuppressive IL-17-producing T regulatory (Tr17) cells into tumors. We evaluated soluble MAdCAM-1 (sMAdCAM-1) as a prognostic biomarker in 1,051 patients from three cohorts: JAVELIN Renal 101 (avelumab plus axitinib versus sunitinib), SURF (sunitinib) and NIVOREN (nivolumab after tyrosine kinase inhibitors). In the JAVELIN cohort, baseline sMAdCAM-1 levels >180 ng ml $^{-1}$ were associated with significantly improved progression-free survival (13.9 versus 8.4 months, $P < 0.01$) and overall survival (18 months: 84.2% versus 68.1%, $P < 0.01$), independent of IMDC risk groups. We validated the prognostic value of sMAdCAM-1 for overall survival in the SURF and NIVOREN cohorts. Notably, low sMAdCAM-1 levels were associated with an immunosuppressive gut microbiota profile dominated by *Enterocloster* species. Therefore, sMAdCAM-1 deserves further investigations as a biomarker-guided tool for microbiota-targeted interventions.

While cancer immunotherapy revolutionized the clinical management of patients with cancer, resistance remains a major challenge¹. The study of biomarkers offers a pathway to decipher immunotherapy resistance, tailoring treatment to each patient's unique profile and tumor biology². Over the past decade, gut microbiota has emerged as a key modulator of the efficacy of immunotherapy^{3–5} and tyrosine kinase inhibitors (TKIs)^{6,7} across cancer types. Studies heralded the deleterious effects of broad-spectrum antibiotics taken around the first administration of the immunostimulatory immune checkpoint inhibitors anti-PD-1, anti-PD-L1 and anti-CTLA-4 monoclonal antibodies on response rates and survival of patients across various

cancer types and immune checkpoint inhibitors (ICIs) regimens (alone or combined with chemotherapy or TKI)^{4,8}. Several factors, including certain comedications (such as antimicrobials), chronic inflammatory diseases and cancer itself, may cause a deviation of the microbial repertoire from healthy intestinal commensalism, a phenomenon known as gut dysbiosis^{9,10}. Notably, prior exposure to TKIs before initiating nivolumab has also been shown to alter the gut microbiota composition, potentially affecting subsequent immunotherapy efficacy¹¹. Gut dysbiosis has been linked to altered gut and blood metabolomes, systemic inflammation and circulating CD8 $^{+}$ T cell exhaustion¹².

Table 1 | Clinical characteristics of the patients from three independent clinical trials

Clinical characteristics	TC (n = 603)	sMAdCAM-1 ^H (n = 461)	sMAdCAM-1 ^L (n = 142)	P value	VC ¹ (n = 278)	sMAdCAM-1 ^H (n = 66)	sMAdCAM-1 ^L (n = 212)	P value	VC ² (n = 170)	sMAdCAM-1 ^H (n = 69)	sMAdCAM-1 ^L (n = 101)	P value	
Age (year)	Median (range)	61 (27–85)	61 (35–81)	0.83	65 (22–87)	64 (33–77)	65 (22–87)	0.18	64 (29–84)	63 (39–79)	64 (29–84)	0.45	
Sex at birth, n (%)	Male	447 (74)	336 (73)	111 (78)	0.25	223 (80)	53 (80)	170 (80)	1	136 (80)	57 (83)	79 (78)	
	Female	156 (26)	125 (27)	31 (22)		55 (20)	13 (20)	42 (20)		34 (20)	12 (17)	22 (22)	
ECOG performance status, n (%)	0–1	603 (100)	461 (100)	142 (100)		228 (86)	62 (95)	166 (83)		163 (96)	68 (100)	95 (94)	
	2 or more	0	0	0		36 (14)	3 (5)	33 (17)		6 (4)	0	6 (6)	
	Not reported	0	0	0		14	1	13		1	1	0	
	<25	190 (32)	138 (30)	52 (37)		124 (46)	30 (47)	94 (46)		54 (32)	19 (28)	35 (35)	
BMI classification (kg m ⁻²), n (%)	(25;30)	224 (37)	169 (37)	55 (39)	0.2	105 (39)	27 (42)	78 (38)		77 (46)	35 (51)	42 (42)	
	≥30	184 (31)	150 (33)	34 (24)		41 (15)	7 (11)	34 (17)		36 (22)	14 (21)	22 (22)	
	Not reported	5	4	1		8	2	6		3	1	2	
	Clear cell	603 (100)	461 (100)	142 (100)		278 (100)	66 (100)	212 (100)		125 (98)	57 (100)	68 (97)	
Tumor histology, n (%)	Non-clear cell	0	0	0		0	0	0		2 (2)	0	2 (3)	
	Not reported	0	0	0		0	0	0		43	12	31	
	Favorable	135 (23)	117 (26)	18 (13)		48 (17)	19 (29)	29 (14)		68 (40)	28 (41)	40 (40)	
IMDC score, n (%)	Intermediate	372 (62)	291 (64)	81 (57)		158 (57)	39 (59)	119 (56)		79 (46)	38 (55)	41 (41)	
	Poor	92 (15)	49 (11)	43 (30)	1.70 × 10 ⁻⁸	71 (26)	8 (12)	63 (30)	0.001	23 (14)	3 (4)	20 (20)	
	Not reported	4	4	0		1	0	1		0	0	0	
	Brain metastasis, n (%)	Yes	4	3	1		27 (10)	7 (11)	20 (10)	0.81	5	3	2
		Not reported	599	458	141		5	1	4		165	66	99
	Liver metastasis, n (%)	Yes	12	11	1		74 (27)	18 (28)	56 (27)		16	4	12
		Not reported	591	450	141		5	1	4		154	65	89
	Bone metastasis, n (%)	Yes	–	–	–		84 (31)	10 (15)	74 (36)	0.002	25	6	19
		Not reported	603	461	142		5	1	4		145	63	82
	Number of previous therapy lines, n (%)	None	603 (100)	603 (100)		0	0	0		170 (100)	69 (100)	101 (100)	
		1	0	0		155 (56)	37 (56)	118 (56)	1	0	0	0	
		≥2	0	0		123 (44)	29 (44)	94 (44)		0	0	0	
Best response, n (%)	CR/PR	291 (49)	229 (50)	62 (44)		48 (18)	11 (17)	37 (19)		81 (50)	36 (55)	45 (47)	
	SD	229 (38)	177 (39)	52 (37)		85 (32)	23 (35)	62 (31)		64 (40)	24 (36)	40 (42)	
	PD	70 (12)	47 (10)	23 (16)	0.13	130 (49)	31 (48)	99 (50)	0.85	17 (10)	6 (9)	11 (11)	
	NCR/NPD	9 (2)	6 (1)	3 (2)		–	–	–		–	–	–	
	Not reported	4	2	2		15	1	14		8	3	5	

TC, training cohort (JAVELIN Renal 010); VC¹, first validation cohort (NIVOREN); VC², second validation cohort cohort (SURF); sMAdCAM-1^H, high values of sMAdCAM-1; sMAdCAM-1^L, low values of sMAdCAM-1; NCR/NPD, noncomplete response or progressive disease; n, number; CR/PR, complete/partial responses; SD, stable disease; PD, progressive disease. P values determined by Fisher test.

Causal links between gut dysbiosis and resistance to cancer immunotherapy have been demonstrated in preclinical models and proof-of-concept clinical trials. Interventions aimed at restoring a favorable microbiota, such as fecal microbial transplantation from patients who benefited from ICI or from healthy volunteers, in individuals with metastatic melanoma^{13–16}, lung cancer¹⁷ and renal cell carcinoma (RCC)^{11,18,19}, or oral administration of the probiotic *Clostridium butyricum* strain CBM 588 in patients with metastatic RCC (mRCC)^{20,21} have yielded encouraging results. These findings have spurred efforts to refine the diagnosis of gut dysbiosis, with the prospect of identifying participants who need to restore intestinal integrity to enhance responses to ICI.

The most comprehensive methodology to assess baseline gut dysbiosis relies on metagenomic shotgun sequencing (MGS) of fecal material^{11,22}. Large MGS datasets have enabled the development of microbiota-based biomarkers based on machine learning²³ or custom scoring based on quantitative polymerase chain reaction²⁴. Unmasking mechanisms by which antibiotics mediate their immunosuppressive effects has led to the discovery of a circulating biomarker, sMAdCAM-1, linked to a specific compositional shift of the intestinal microbiota and clinical outcomes in patients with lung cancer and genitourinary cancers²⁵. Indeed, the relative overdominance of the genus *Enterocloster* induces the downregulation of MAdCAM-1 in high endothelial venules of the ileal lamina propria and mesenteric lymph nodes, leading to migration and tumor homing of enterotropic interleukin-17 (IL-17)-producing immunosuppressive T cells, which express the $\alpha 4\beta 7$ heterodimeric MAdCAM-1 receptor²⁵. Notably, MAdCAM-1 is shed into the blood with sMAdCAM-1 levels reflecting the ileal expression of MAdCAM-1 (ref. 25). Remarkably, low sMAdCAM-1 levels were associated with poorer prognosis in three independent cohorts of patients with cancer treated with ICI-based regimens after first line of therapy²⁵.

In the current work, we asked whether sMAdCAM-1 levels could serve as a biomarker of an immunosuppressive microbiota linked to resistance to ICI and/or TKI regimens, specifically in patients with mRCC. We investigated the distribution and biological significance of baseline and on-treatment sMAdCAM-1 levels in the following three independent cohorts of patients with mRCC: the JAVELIN Renal 101 trial (NCT02684006)^{26,27}, the SURF trial (NCT02689167)²⁸ and the GETUG-AFU26-NIVOREN trial (NCT03013335)²⁹.

Results

Distribution of sMAdCAM-1 in individuals with mRCC compared with controls

We measured sMAdCAM-1 levels using a Luminex assay in two independent cohorts of healthy volunteers. The first was the Weill Cornell Medicine Employees (WELCOME) cohort, comprising 75 healthcare workers from Weill Cornell Medicine in the USA (median age = 42 years, range = 26–75; predominantly female (76%))³⁰. The second was the Belgian Flemish study on Environment, Genes and Health Outcomes (FLEMENGHO) cohort, including 49 healthy individuals (median age = 63 years, range = 59–66; predominantly male (56%))³¹. The training cohort consisted of patients included in the phase 3 randomized JAVELIN Renal 101 trial (NCT02684006) with available plasma samples (68% of the intent-to-treat population). Overall, patients were mostly male (74%), with a median age of 61 (27–85) years and of intermediate International Metastatic RCC Database Consortium (IMDC) risk (62%; Table 1 and Extended Data Fig. 1a). All patients had an Eastern Cooperative Oncology Group (ECOG 0–1) and clear-cell histology. The median follow-up was 18.9 months. The validation cohorts comprised the following two prospective phase 2 trials: SURF (NCT02689167), a prospective trial that evaluated two different sunitinib schedule modifications in patients with mRCC experiencing sunitinib-related toxicity; NIVOREN (NCT03013335), a prospective real-world setting study of nivolumab after antiangiogenic TKI. In the NIVOREN cohort, patients were mostly male (80%), with a median age of 65 years (range = 22–87) and ECOG

0–1 (86%). In the SURF cohort, patients were mostly male (80%), with a median age of 64 years (range = 29–84) and ECOG 0–1 (96%).

The median sMAdCAM-1 concentrations were 196 and 178 ng ml⁻¹ in the WELCOME and FLEMENGHO cohorts, respectively, with no significant difference between the two ($P = 0.3173$; Fig. 1a). The median value of sMAdCAM-1 was 187 ng ml⁻¹ for all healthy volunteers (both WELCOME and FLEMENGHO cohorts merged). In patients with mRCC enrolled in the JAVELIN Renal 101 trial (Extended Data Fig. 1a), the median values of sMAdCAM-1 at baseline were 234 and 238 ng ml⁻¹ for the avelumab + axitinib and for the sunitinib arms, respectively (Fig. 1b). In patients with mRCC enrolled in the SURF and NIVOREN trials (Extended Data Fig. 1b,c), the median values of sMAdCAM-1 were 169 and 139 ng ml⁻¹, respectively (Fig. 1c). Patients with refractory mRCC had lower sMAdCAM-1 levels at baseline compared with patients treated in the first-line setting and healthy volunteers (Fig. 1d). Additionally, we observed increased proportions of patients presenting low sMAdCAM-1 levels (<180 ng ml⁻¹) in the poor IMDC risk factor group compared with patients in the favorable or intermediate IMDC risk groups (Fig. 1e; $P = 0.0003$ for avelumab + axitinib arm and $P < 0.0001$ for sunitinib arm). In line with this finding, sMAdCAM-1 levels also correlated with the main circulating inflammatory cytokines, IL-6 and IL-8 ($P < 0.001$ and $P = 0.010$, respectively; Fig. 1f,g). A weak correlation between age and baseline sMAdCAM-1 levels was also observed (Spearman's $\rho = 0.15$, $P = 0.09$) in the training cohort, while no correlation was observed in the NIVOREN (Spearman's $\rho = -0.06867$ and $P = 0.2538$) or SURF (Spearman's $\rho = 0.00144$, $P = 0.9847$) validation cohorts, using single-agent nivolumab and single-agent sunitinib, respectively. Moreover, sMAdCAM-1 and the estimated glomerular filtration rates were positively and very weakly correlated (Spearman's $\rho = 0.16$, $P = 0.03$).

These findings suggest that lower sMAdCAM-1 levels may be associated with advanced mRCC and dismal prognosis.

Low levels of sMAdCAM-1 are associated with reduced survival in the training cohort. The optimal cut-off was 180 ng ml⁻¹ (25% percentile) based on the overall survival (OS) outcome in the whole population. Restricted cubic spline and residual plots further confirmed a non-linear relationship of sMAdCAM-1 levels with OS (Extended Data Fig. 2). Notably, the population included in the sMAdCAM-1 analysis was comparable to the intent-to-treat population in terms of survival outcomes (Extended Data Fig. 3a).

Overall, patients who had higher sMAdCAM-1 levels (>180 ng ml⁻¹) experienced improved progression-free survival (PFS; median = 13.9 (11.3, 16.6) versus 8.4 (6.0, 9.9) months, $P < 0.01$) and OS (median = not reached (NR) (30.0, NR) versus 24.6 (22.2, NR) months; 18-month OS rates were 84.2% (80.2%, 87.4%) versus 68.1% (59.2%, 76.5%), $P < 0.01$; Extended Data Fig. 3a,b). These associations remained significant after adjusting for IMDC risk groups (Extended Data Table 1). The survival advantage of high sMAdCAM-1 levels was independent of study arm—median PFS was 18.0 (13.4, 21.0) versus 8.7 (6.0, 13.8) months and 18-month OS rates were 85.2% (79.6%, 89.3%) versus 75.6% (64.0%, 84.0%) for the avelumab + axitinib arm (Fig. 2a,b); median PFS was 11.1 (8.6, 13.9) versus 6.9 (5.6, 11.1) months and 18-month OS rates were 83.2% (77.1%, 87.8%) versus 58.6% (44.3%, 70.5%) for the sunitinib arm (Fig. 2c,d; $P_{\text{interaction}} = 0.798$ and 0.370 for PFS and OS, respectively). The prognostic model incorporating IMDC + sMAdCAM-1 demonstrated a significant improvement in the area under the curve (AUC) at 18 months compared to the IMDC model alone (0.72 versus 0.68; $P = 0.01$; Extended Data Table 1).

We conclude that sMAdCAM-1 < 180 ng ml⁻¹ is a negative prognostic biomarker in patients with mRCC treated with first-line therapy, irrespective of the systemic treatment.

Low levels of sMAdCAM-1 are associated with reduced OS in the validation cohorts. The percentage of patients with mRCC presenting with sMAdCAM-1 < 180 ng ml⁻¹ was 59% and 76% in the validation SURF

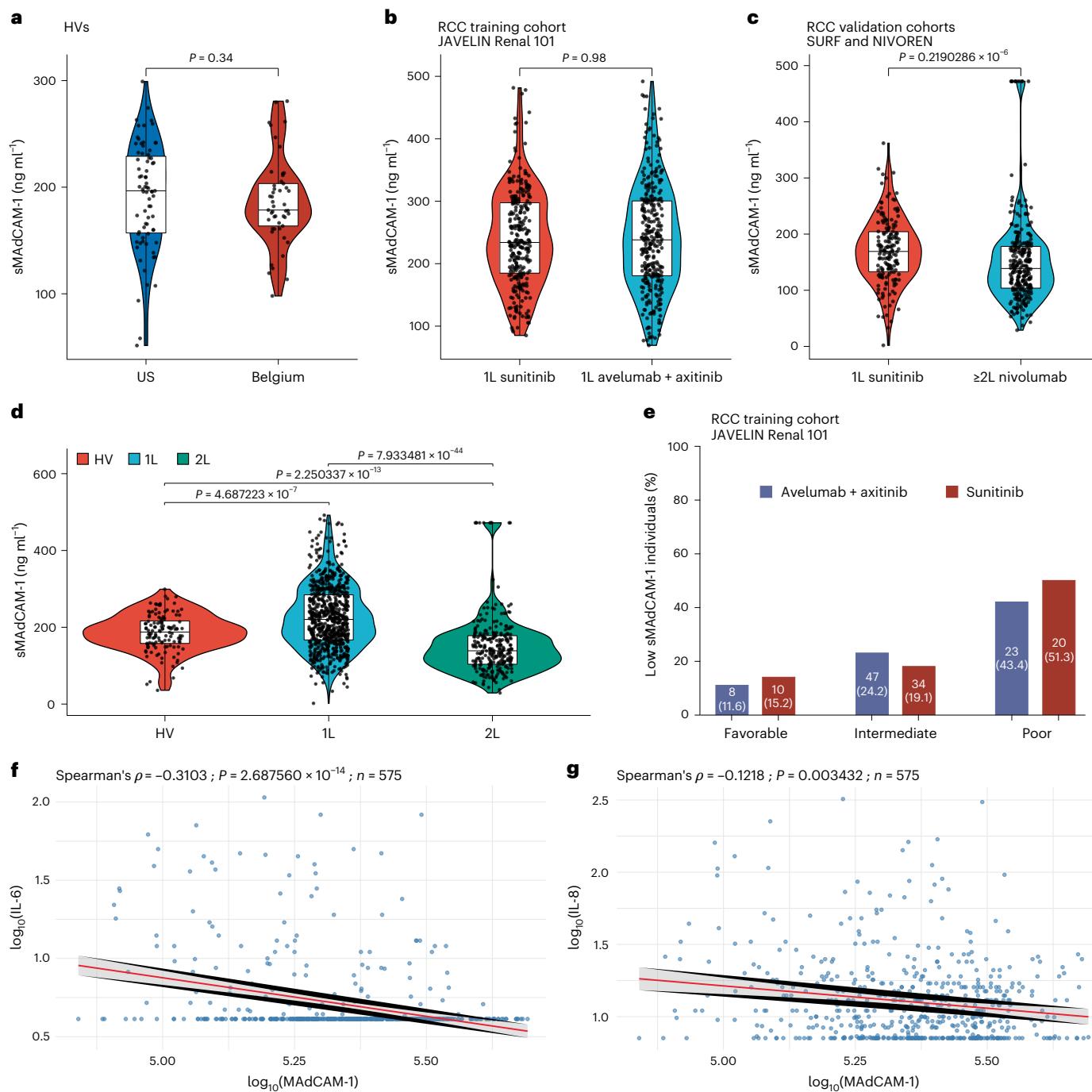


Fig. 1 | Distribution of sMAdCAM-1 levels in patients with mRCC cohorts compared to healthy volunteers. **a–c**, Violin plots with overlaid boxplots showing the distribution of sMAdCAM-1 concentrations across cohorts of healthy volunteers (HVs) from the USA ($n = 75$) and Belgium ($n = 49$; **a**), in the training cohort of patients treated with first-line sunitinib ($n = 284$) or first-line axitinib plus avelumab ($n = 319$; **b**) and in the validation cohorts of patients treated with first-line sunitinib ($n = 170$) or second-line or later-line nivolumab ($n = 278$; **c**). The box bounds are the Q1, median, and Q3; the whiskers show $Q1 - 1.5 \times$ the IQR and $Q3 + 1.5 \times$ the IQR. Statistical comparisons between groups were performed using a two-sided Wilcoxon rank-sum test without adjustments for multiple comparisons; exact P values are shown. **d**, Violin plots with overlaid boxplots showing the distribution of sMAdCAM-1 concentrations across healthy volunteers ($n = 124$) and patients

treated with first-line (1L) or second-line (2L) therapies ($n = 1,051$). The box bounds are the Q1, median, and Q3; the whiskers show $Q1 - 1.5 \times$ the IQR and $Q3 + 1.5 \times$ the IQR. Statistical comparisons between groups were performed using a two-sided Wilcoxon rank-sum test without adjustments for multiple comparisons; exact P values are shown. **e**, Bar plots show the number and percentage (in parentheses) of individuals with low sMAdCAM-1 concentrations ($\leq 180 \text{ ng ml}^{-1}$) by IMDC risk group in the training cohort. **f,g**, Scatterplots showing the relationship between MAdCAM-1 concentrations and IL-6 (**f**) and IL-8 (**g**) in plasma samples. Each point represents an individual sample measurement. The solid line represents the linear regression fit, with the shaded area representing the 95% CI of the fitted regression line. Statistical comparisons between groups were performed using a two-sided Spearman test without adjustments for multiple comparisons; exact P values are shown.

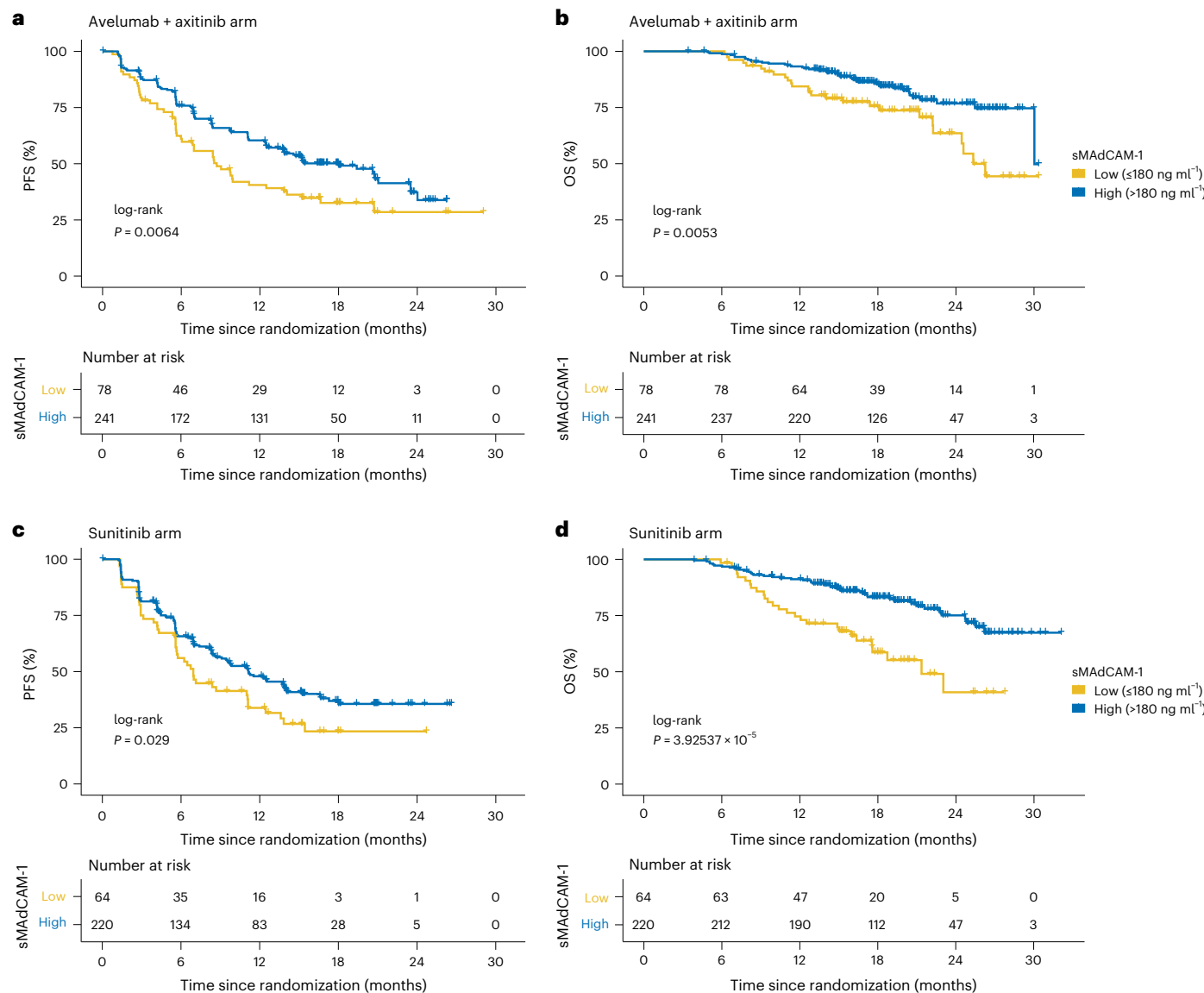


Fig. 2 | Low levels of sMAdCAM-1 are associated with reduced survival in the Javelin Renal 101 trial (training cohort). a–d, Kaplan–Meier survival estimates of PFS (a,c) and OS (b,d) in patients treated with avelumab plus axitinib (a,b) or with sunitinib (c,d), stratified by sMAdCAM-1 concentrations in the training

cohort. Patients were dichotomized using a threshold of 180 ng ml^{-1} into low ($\leq 180 \text{ ng ml}^{-1}$) and high ($> 180 \text{ ng ml}^{-1}$) sMAdCAM-1 groups. Survival differences were assessed using the log-rank test; P values are shown. Risk tables indicate the number of patients at risk at each time point.

and NIVOREN cohorts, respectively. The SURF cohort included two patients with nonclear cell histology, both of whom were in the low sMAdCAM-1 group. The low sMAdCAM-1 group had a higher proportion of patients with ECOG ≥ 2 ($P = 0.04$) and a poor-risk IMDC group ($P < 0.01$). In the NIVOREN cohort, these patients also had more bone metastatic sites at study inclusion ($P = 0.002$). The median follow-up was 34 (1.0, 70.0) and 21.8 (20.2, 22.7) months in the SURF and NIVOREN cohorts, respectively. Patients with higher sMAdCAM-1 levels had a numerical OS advantage—NR (1.0, 59.0) versus 50 (2.0, 70.0) months ($P = 0.0565$, log rank) in the SURF cohort and NR (23.7, NR) versus 18.8 (14.6, 24.1) months ($P = 0.0004$, log rank) in the NIVOREN cohort (Fig. 3a,b). However, sMAdCAM-1 levels did not significantly impact PFS in either cohort (Extended Data Fig. 4a,b).

The multivariable Cox regression analysis in the NIVOREN cohort ($n = 263$) revealed that low baseline sMAdCAM-1 levels (< 180) were independently associated with worse OS in nivolumab-treated patients, demonstrating a significant hazard ratio (HR) of 2.11 (95% confidence interval (CI) = 1.27–3.49; Extended Data Table 2). Hence, patients with

sMAdCAM-1 below this threshold doubled their risk of death compared to those with higher levels, even after adjusting for other relevant clinical variables such as antibiotic intake or IMDC. Interestingly, while prior antibiotic use showed a nonsignificant trend toward poorer outcomes (HR = 1.44; 95% CI = 0.90–2.31), it did not reach statistical significance in this model. Furthermore, the interaction analysis between sMAdCAM-1 and antibiotic use was nonsignificant ($P = 0.1005$), indicating that the prognostic value of sMAdCAM-1 was consistent regardless of patients' antibiotic exposure history. The potential links between toxicity events and sMAdCAM-1 could not be studied, either due to data unavailability (JAVELIN Renal 101) or low frequencies (SURF, NIVOREN).

Hence, we validated the sMAdCAM-1 (using the 180 ng ml^{-1} cut-off value defined in the training cohort) as a prognostic biomarker for OS in patients with mRCC receiving first-line or subsequent therapy, across both ICI and TKI monotherapy regimens.

Immunotherapy increases sMAdCAM-1 levels. We next analyzed longitudinally the evolution of sMAdCAM-1 as a dynamic biomarker

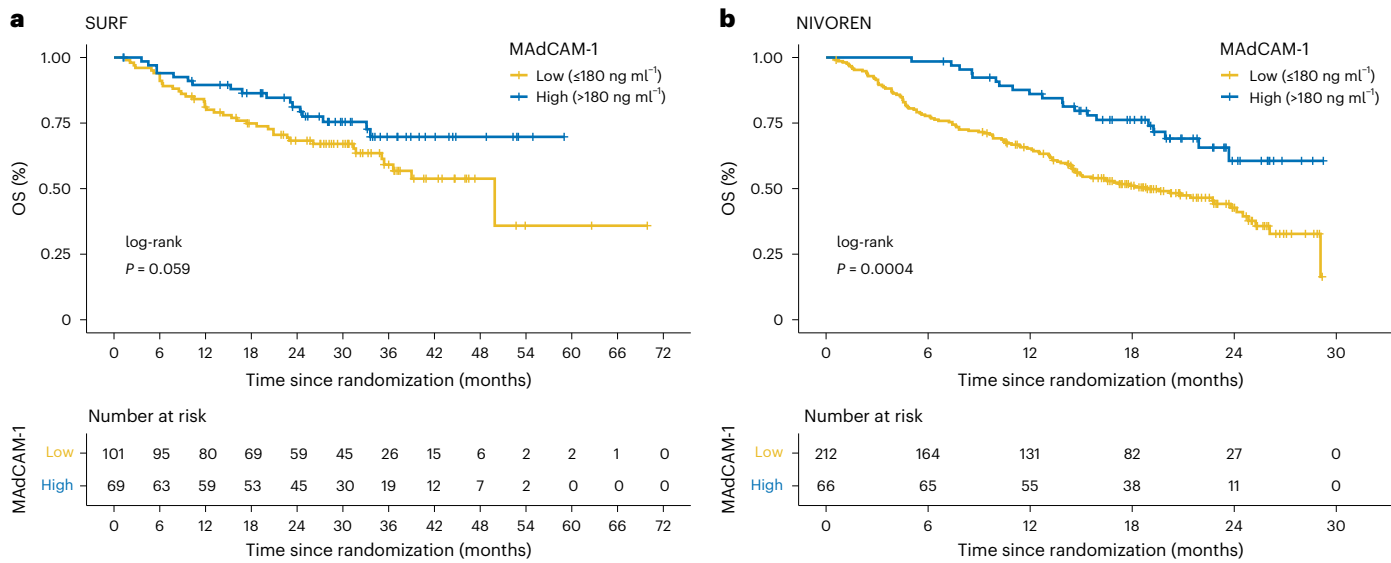


Fig. 3 | The prognostic impact of sMAdCAM-1 is validated in the SURF and NIVOREN trials (validation cohorts). a,b, Kaplan–Meier survival estimates of OS stratified by sMAdCAM-1 concentrations in the SURF (a) and NIVOREN (b) validation cohorts. Patients were dichotomized using a threshold of 180 ng ml⁻¹

into low (≤ 180 ng ml $^{-1}$) and high (> 180 ng ml $^{-1}$) sMAdCAM-1 groups. Survival differences were assessed using the log-rank test; *P* values are shown. Risk tables indicate the number of patients at risk at each time point.

while on TKI alone (sunitinib arm) or TKI combined with ICI (avelumab plus axitinib arm) in the JAVELIN Renal 101 trial and during ICI alone (nivolumab) in the NIVOREN trial. After 12 weeks of therapy (C3 visit), the circulating levels of sMAdCAM-1 decreased from a median of 234 down to 213 ng ml $^{-1}$ in the sunitinib arm (Fig. 4a, left; *P* = 0.0021), while they increased from 238 to 270 ng ml $^{-1}$ in the avelumab plus axitinib arm (Fig. 4a, right; *P* < 0.0001). The latter finding was corroborated in the NIVOREN validation cohort after 24 weeks of therapy (C7 visit; Fig. 4b; *P* < 0.001). We also noted that sMAdCAM-1 levels decrease at progression (Fig. 4b; *P* = 0.035).

Furthermore, we observed different sMAdCAM-1 dynamics in the two arms of the JAVELIN Renal 101 trial (*P* < 0.001; Fig. 4c). sMAdCAM-1 levels remained below our defined threshold after the first two cycles of treatment (C1 ≤ 180 and C3 ≤ 180) in 17.6% of patients in the sunitinib arm compared to 7.5% of those treated with the ICI-based combination (low–low; Fig. 4c). Indeed, up to 16.9% of patients with mRCC treated with avelumab + axitinib normalized their sMAdCAM-1 levels after initiation of therapy (C1 ≤ 180 and C3 > 180), versus 4.9% in the sunitinib arm (low–high; Fig. 4c). Moreover, 14.4% of the patients treated in the sunitinib arm experienced a decrease in their sMAdCAM-1 versus 5.3% in the avelumab + axitinib arm (high–low; Fig. 4c). The persistent low sMAdCAM-1 level translated into worse survival in the Javelin Renal 101 trial regardless of treatment arm, for both PFS and OS (Fig. 4d,e and Extended Data Table 3; *P*_{interaction} = 0.88 and 0.16 for PFS and OS, respectively).

We conclude that low sMAdCAM-1 at baseline and after two cycles of therapy are negative prognostic biomarkers in patients with mRCC regardless of treatment regimen.

The gut microbiota composition is dynamically influenced by cancer therapies. To investigate potential links between low sMAdCAM-1 levels and gut dysbiosis, we performed MGS of stool samples from individuals living with RCC in the prospective ONCOBIMOTICS study at baseline and following TKI or ICI therapies.

In 37 TKI-treated patients, we observed a trend toward reduced microbial diversity (richness and species abundances), reflected in decreased Shannon index values post-treatment (Fig. 5a; *P* = 0.08). TKI therapy induced relative overgrowth of immunosuppressive

Enterocloster species (*Enterocloster aldensis*, *Enterocloster citroniae* and *Enterocloster bolteae*), prototypical of gut dysbiosis caused by antibiotics^{9,11}, cancer progression^{24,32} or ileal MAdCAM-1 downregulation²⁵. This shift coincided with depletion of immunogenic taxa, including *Lachnospiraceae* family members (*Dorea longicatena*), *Candidatus Cibio bacter quicibialis*²⁴, *Oscillospiraceae* (*Faecalibacterium prausnitzii*³³ and *Ruminococcaceae* unclass.) family members associated with favorable immunogenic properties^{24,32,34}, *Bifidobacterium longum* and *B. adolescentis* associated with response to immunotherapy³⁵ or *Christensenellaceae bacterium NS/64* associated with the abscopal effects of radiotherapy³⁶ (Fig. 5a,b). Conversely, ICI-treated patients (*n* = 78) showed progressive loss of *E. citroniae*, *Clostridium leptum* and *Ruminococcus torques* in responders^{9,11} (Fig. 5c, top), whereas nonresponders lost immunogenic commensals (*Lachnospiraceae bacterium* and *F. prausnitzii*; Fig. 5c, bottom).

Building upon prior findings in 72 patients with non-small cell lung cancer (NSCLC)²⁵, we confirmed that low sMAdCAM-1 correlates with reduced microbial diversity (richness, *P* = 0.04; Shannon index, *P* = 0.05; Fig. 5d) in a larger cohort of 188 patients with NSCLC. Linear discriminant analysis (LDA) effect size analysis further highlighted tolerogenic *Enterocloster* spp.^{9,25} enrichment in patients with low sMAdCAM-1 (Fig. 5e; *Enterocloster* SGB14313, *P* = 0.005; Extended Data Table 4). To validate the *Enterocloster* genus as a cancer-associated dysbiosis marker, we analyzed the ONCOBIOME meta-cohort^{32,37} (*n* = 457 patients with NSCLC, RCC, bladder³², colorectal^{32,38} and hematological malignancies³⁹) with MGS in stool samples paired with sMAdCAM-1 in the plasma samples. Using a previously defined ratio (S score) between species-interacting groups ('SIG'; 37 SIG1 taxa linked to poor outcome (OS < 12 months); 45 SIG2 taxa associated with OS > 12 months)²⁴, we found that distinct *Enterocloster* species best discriminated ≥ 9 SIG1 counts from < 9 SIG1 counts individuals (Fig. 5f). In the mRCC cohort (*n* = 174), patients with high SIG1 commensals counts (≥ 9 , threshold defined as the median SIG1 count in the ONCOBIOME metacohort) showed worse OS than those with low SIG1 counts (*n* = 174; Fig. 5g, top; *P* = 0.030). In fact, we observed a weak but significant inverse correlation between sMAdCAM-1 and SIG1 abundance (Fig. 5g, bottom; *P* = 0.02). Consistently, sMAdCAM-1 inversely correlated with *Enterocloster* SGB14313 abundance across cohorts (*n* = 55 patients

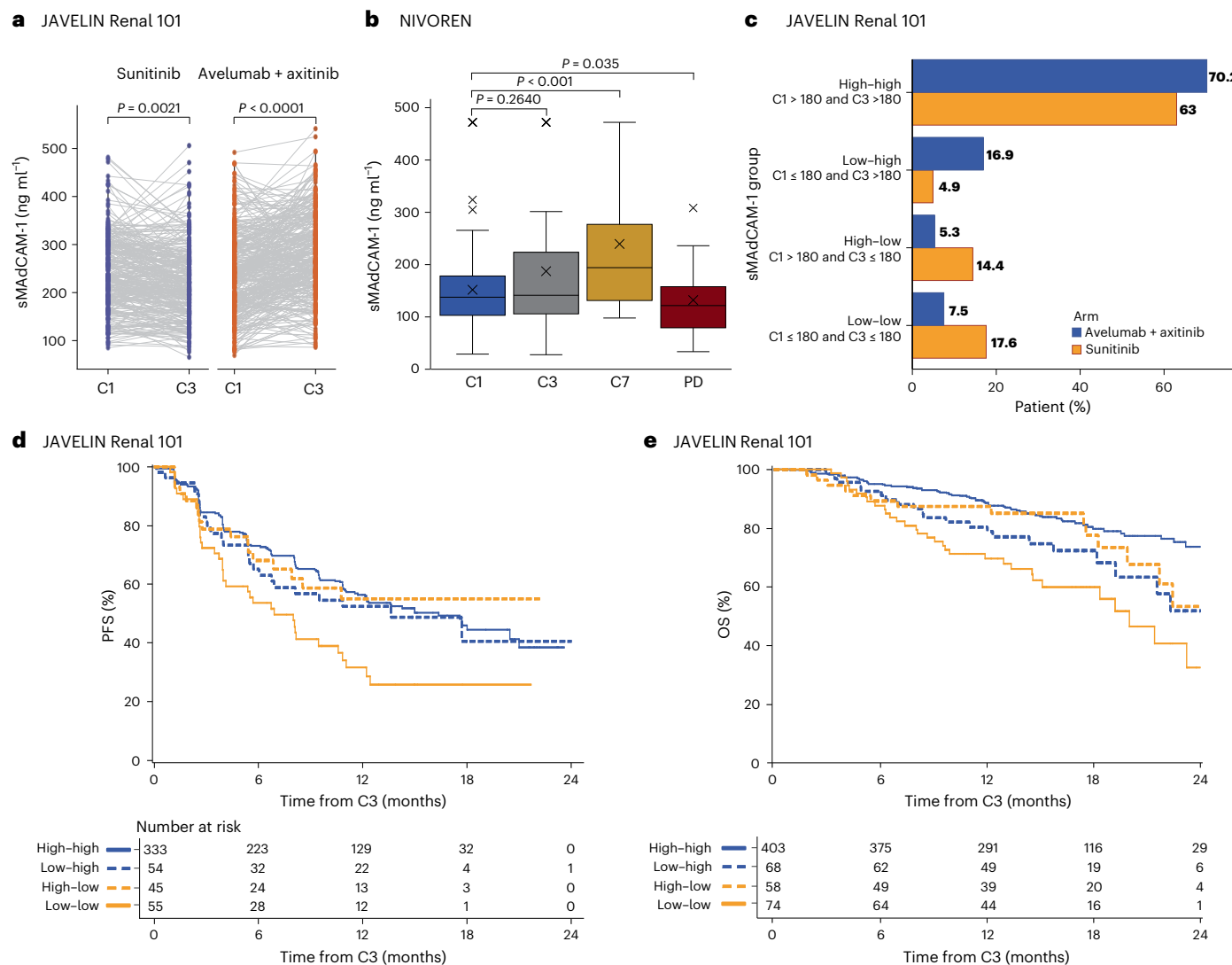


Fig. 4 | Pharmacodynamics of sMAdCAM-1 during treatment. **a**, Paired dot plots showing plasma MAdCAM-1 concentrations at baseline (C1) and on therapy (C3) for individual patients in each treatment arm (sunitinib, $n = 284$; avelumab + axitinib, $n = 319$). Filled circles are colored by treatment arm. Data were analyzed using a two-sided paired t -test; P values are indicated. **b**, Boxplots showing the longitudinal distribution of sMAdCAM-1 concentrations in the NIVOREN at C1 ($n = 278$), C3 ($n = 80$), C7 ($n = 27$) and disease progression (PD; $n = 23$). The box bounds are the Q1, median and Q3; the whiskers show Q1 $- 1.5 \times$ the IQR and Q3 $+ 1.5 \times$ the IQR. 'X' represents the mean, and the small 'x' denotes extreme values. Statistical comparisons between groups were performed using a two-sided Wilcoxon rank-sum test. P values are shown. **c**, Horizontal bar

plot showing the distribution of patients across four longitudinal sMAdCAM-1 categories, defined by dichotomized values at baseline (C1) and on-treatment (C3) using a threshold of 180 ng ml^{-1} : low-low, low-high, high-low and high-high. Categories reflect changes in sMAdCAM-1 status over time. Bars represent the proportion of patients in each category relative to the total patients in each arm. **d,e**, Kaplan-Meier survival estimates of PFS (d) and OS (e) across four longitudinal sMAdCAM-1 categories, defined by dichotomized values at baseline (C1) and on-treatment (C3) using a threshold of 180 ng ml^{-1} : low-low, low-high, high-low and high-high. Categories reflect changes in sMAdCAM-1 status over time. Risk tables indicate the number of patients at risk at each time point.

with mRCC, $\rho = -0.28$, $P = 0.052$; $n = 61$ patients with bladder cancer, $\rho = -0.21$, $P = 0.099$; $n = 188$ patients with NSCLC, $\rho = -0.15$, $P = 0.049$; Extended Data Fig. 5a–c).

In summary, these findings suggest that sMAdCAM-1 may serve as a surrogate marker for distinct gut microbial profiles relevant to ICI response, particularly reflecting the immunosuppressive *Enterocloster* genus dominance. Further investigation of its utility for guiding microbiota-modulating therapies is warranted.

Discussion

Functional biomarkers to guide meaningful changes in the clinical management of patients with mRCC are needed to predict and/or circumvent resistance to current ICI-based therapeutic regimens. Here we show that a gut immune checkpoint, the MAdCAM-1, known to regulate

the gut homing and exodus of immune cells to the tumor microenvironment, may inform an individualized approach to therapy. In the large multicenter randomized JAVELIN Renal 101 trial of 603 patients with mRCC and available biomarker data, as well as in two additional prospective phase 2 validation cohorts (NIVOREN, $n = 278$; and SURF, $n = 170$), baseline sMAdCAM-1 levels below 180 ng ml^{-1} were associated with reduced OS. Interestingly, the optimal cut-off defined in the training cohort was comparable to the median values in the two healthy volunteer cohorts. Moreover, persistence of sMAdCAM-1 levels below 180 ng ml^{-1} after two treatment cycles was associated with poor prognosis. In a multivariable analysis comprising antibiotic uptake, sMAdCAM-1 remained an independent prognostic biomarker for ICI treatment, beyond the IMDC risk score. This finding corroborates previous reports linking sMAdCAM-1 levels below each cohort's median

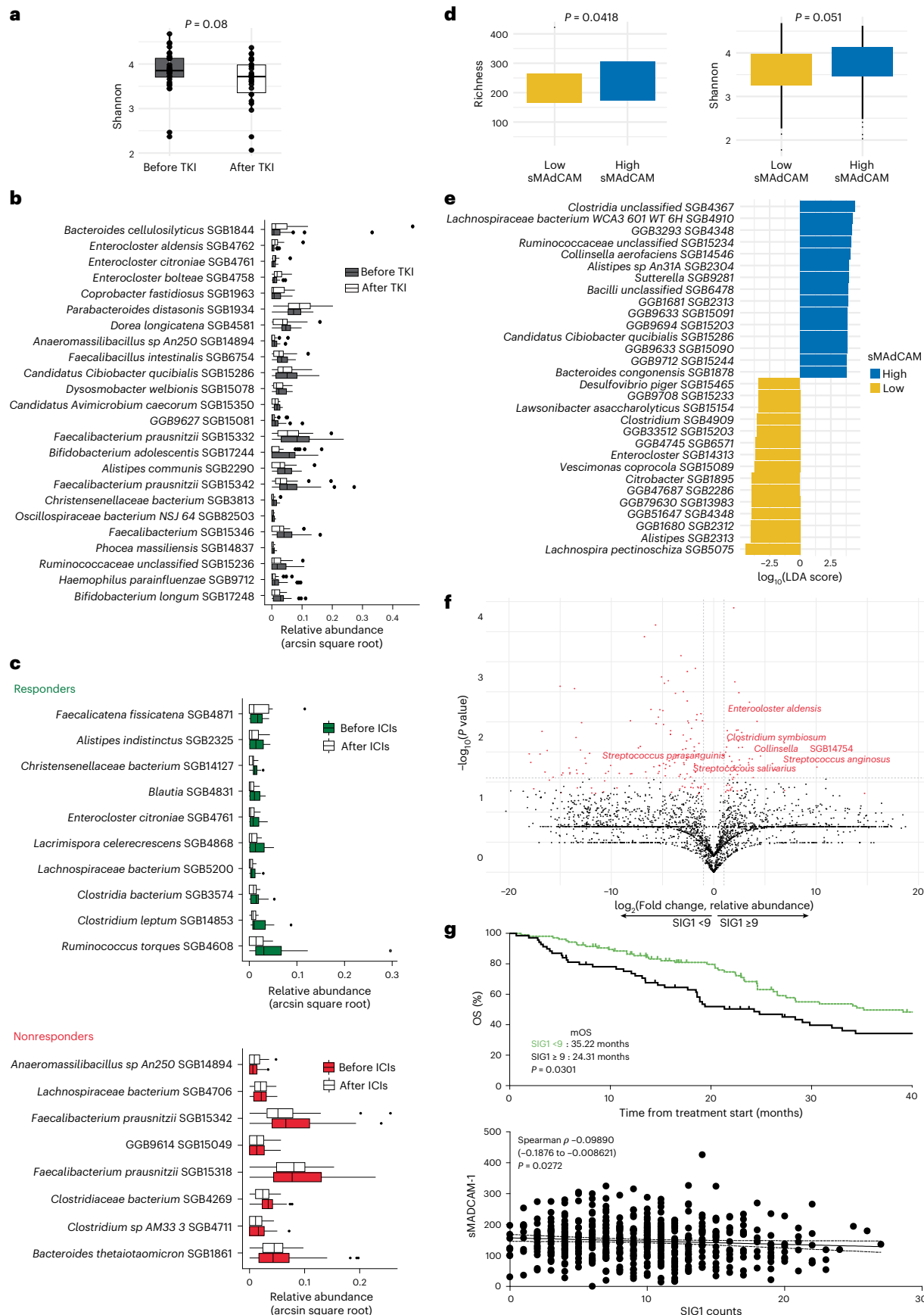


Fig. 5 | Patients with advanced RCC can develop gut dysbiosis during therapy. **a**, Alpha diversity as determined by the Shannon index assessed at baseline and after administration of TKIs alone in $n = 37$ patients with advanced RCC. Boxplots represent the within-category microbial richness distribution summarized by the first and third quartiles as hinges of the box, the median and whiskers extending for the largest or smallest value not exceeding $1.5 \times$ IQR from the two ends of the box, with data beyond these values plotted individually as outliers. Statistical significance was assessed using a two-sided Wilcoxon signed-rank test without adjustments for multiple comparisons. **b,c**, Longitudinal analysis of microbial features in stool samples via MGS. **b**, Paired comparison of baseline versus post-TKI stool samples from the same patients ($n = 37$). **c**, Paired comparison of pre- and post-ICI samples in responders (top; $n = 17$) and nonresponders (bottom; $n = 61$). Response was defined as complete or partial response lasting >12 months with OS >24 months (responders) or progressive disease as best response (nonresponders). Statistical significance was assessed using a two-sided Wilcoxon signed-rank test (features required in ≥ 10 samples per group). Displayed features are filtered for $\geq 50\%$ prevalence in both groups and a raw $P < 0.05$. No associations remained significant after Benjamini–Hochberg correction (false discovery rate (FDR) < 0.2). **d**, Alpha diversity as determined by the richness (left) and Shannon index (right) in patients with advanced NSCLC ($n = 176$) stratified by sMAdCAM-1 levels—low sMAdCAM-1 versus high sMAdCAM-1. Boxplots represent the within-category microbial richness distribution summarized by the first and third quartiles as hinges of the box, the

median and whiskers extending for the largest or smallest value not exceeding $1.5 \times$ IQR from the two ends of the box, with data beyond these values plotted individually as outliers. Statistical significance was assessed using a two-sided Wilcoxon signed-rank test without adjustments for multiple comparisons. **e**, LDA effect size graph was generated using paired sMAdCAM-1 and MGS data in patients with advanced NSCLC ($n = 176$) stratified by sMAdCAM-1 levels—low sMAdCAM-1 and high sMAdCAM-1. See Extended Data Table 4. **f**, Volcano-plot based on MGS showing differences ($P < 0.05$, two-sided Mann–Whitney U -test without adjustments for multiple comparisons) between ≥ 9 SIG1 counts and < 9 SIG1 counts groups ($n = 285$ patients with NSCLC, RCC and bladder cancer). **g**, Kaplan–Meier survival estimates of OS stratified by SIG1 counts in patients with advanced RCC (top). Patients were dichotomized using a threshold ≥ 9 SIG1 counts ($n = 69$, solid line) and < 9 SIG1 counts ($n = 105$, dotted line) groups. Survival differences were assessed using the log-rank test without adjustments for multiple comparisons; exact P values are shown. Scatterplots showing the relationship between sMAdCAM-1 concentrations in plasma samples and SIG1 counts in paired stool samples ($n = 499$; bottom). Each point represents an individual sample measurement. The solid line represents the linear regression fit, with the dotted lines representing the 95% CI of the fitted regression line. Statistical comparisons between groups were performed using a two-sided Spearman test without adjustments for multiple comparisons; exact P values are shown.

values with reduced OS in patients with lung, RCC and urothelial cancer treated after first-line therapy²⁵.

MAdCAM-1 is constitutively expressed in high endothelial venules of the lamina propria, mesenteric lymph nodes and Peyer patches (as well as in the hepatic endothelium of inflamed livers)⁴⁰, can be upregulated during inflammation and shed into the plasma in conditions that remain unclear. Loss of the MAdCAM-1 protein parallels the loss of FOXP3 regulatory T (T_{reg}) cells and IL-17-producing ROR γ T CD4 $^{+}$ T cells in the lamina propria²⁵. In experimental models, we showed a cause-and-effect relationship between high expression (and shedding) of MAdCAM-1 in the liver and the interception of the migration of enterotropic T_{reg} cells to tumor lesions²⁵. Other reports highlighted the relevance of the MAdCAM-1- $\alpha 4\beta 7$ tropism during chronic inflammatory processes within or outside the intestines^{41–43}. Ileal endothelial MAdCAM-1 is downregulated during gut dysbiosis following broad-spectrum antibiotics or tumor progression in mice and patients²⁵. However, fecal microbial transplantation using a healthy microbiota or specific commensal strains can restore MAdCAM-1 expression on the surface of ileal endothelial cells. Indeed, *Akkermansia* species (in particular *Akkermansia massiliensis* SGB9228) markedly upregulated MAdCAM-1 expression levels after an oral gavage performed postantibiotic therapy²⁵. Moreover, our group recently showed that the combination of low sMAdCAM-1 levels and the absence of fecal *Akkermansia* species identified a subgroup of patients with metastatic colorectal cancer resistant to immunochemotherapy³². Notably, here we show that TKI therapy was associated with an overgrowth in the population of immunosuppressive genus *Enterocloster*, a finding also seen in individuals who do not respond to ICI^{24,44,45} or are diagnosed with chronic inflammatory disorders^{10,46}. These findings suggest that patients with mRCC and low sMAdCAM-1 levels may benefit from microbiota-centered interventions. In certain RCC cohorts, this can represent up to 76% of patients. Two pioneering randomized studies^{7,20,47} provided the proof-of-concept that a Japanese probiotic *Clostridium butyricum* MIYAIRI 588 (CBM588) can enhance the efficacy of ICIs or TKI + ICI combinations. The first clinical study randomizing TKI + ICI with or without FMT met its primary endpoint to improve PFS in patients with IMDC intermediate or poor when transferring an exogenous microbiota from a patient with mRCC and achieved durable benefit on ICI among treatment-naïve patients¹⁸. A phase 1 clinical trial (NCT05865730) is currently underway, evaluating the impact of daily administration of Oncobax AK—a capsule containing live *A. massiliensis* (strain p2261, SGB9228), which

shares overlapping health-related functions with *Akkermansia muciniphila*—in patients with mRCC who are *Akkermansia*-deficient at the initiation of the first-line therapy⁴⁸.

This study has several limitations. First, conclusions are derived from clinical trials with strict eligibility criteria, potentially limiting generalizability to real-world populations. Second, we could not account for comorbidities that may influence microbiome composition, including inflammatory bowel disease (Crohn's disease and ulcerative colitis), prior bowel resections or use of over-the-counter probiotics. Third, while adding sMAdCAM-1 to prognostic models significantly improved survival prediction (AUC = 0.72 versus 0.68), its absolute incremental value remains modest. Although mechanistically linked to IMDC and IL-6 pathways, the biomarker's clinical utility may be greatest within microbiota-directed therapeutic strategies rather than as a standalone prognostic tool. Finally, the cohorts included therapies that have become less relevant to contemporary management of patients with mRCC (avelumab, nivolumab monotherapy), further limiting their current clinical applicability.

Altogether, these findings support a paradigm shift in the management of mRCC, highlighting the need for biomarker-guided clinical trials investigating microbiota-targeted interventions aimed at enhancing the efficacy of standard ICI-based therapies.

Online content

Any methods, additional references, Nature Portfolio reporting summaries, source data, extended data, supplementary information, acknowledgements, peer review information; details of author contributions and competing interests; and statements of data and code availability are available at <https://doi.org/10.1038/s41591-025-04067-x>.

References

1. Ribas, A. & Wolchok, J. D. Cancer immunotherapy using checkpoint blockade. *Science* **359**, 1350–1355 (2018).
2. Li, H., Van Der Merwe, P. A. & Sivakumar, S. Biomarkers of response to PD-1 pathway blockade. *Br. J. Cancer* **126**, 1663–1675 (2022).
3. Zitvogel, L., Ma, Y., Raoult, D., Kroemer, G. & Gajewski, T. F. The microbiome in cancer immunotherapy: diagnostic tools and therapeutic strategies. *Science* **359**, 1366–1370 (2018).
4. Derosa, L. et al. Microbiota-centered interventions: the next breakthrough in immuno-oncology?. *Cancer Discov.* **11**, 2396–2412 (2021).

5. Routy, B. et al. Melanoma and microbiota: current understanding and future directions. *Cancer Cell* **42**, 16–34 (2024).
6. Alves Costa Silva, C. et al. 1452MO longitudinal analysis reveals gut microbiota shift during standard therapies in metastatic renal cell carcinoma (mRCC). *Ann. Oncol.* **33**, S1208 (2022).
7. Dizman, N. et al. Randomized trial assessing impact of probiotic supplementation on gut microbiome and clinical outcome from targeted therapy in metastatic renal cell carcinoma. *Cancer Med.* **10**, 79–86 (2021).
8. Elkrief, A. et al. Antibiotics are associated with worse outcomes in lung cancer patients treated with chemotherapy and immunotherapy. *NPJ Precis. Oncol.* **8**, 143 (2024).
9. Yonekura, S. et al. Cancer induces a stress ileopathy depending on β -adrenergic receptors and promoting dysbiosis that contributes to carcinogenesis. *Cancer Discov.* **12**, 1128–1151 (2022).
10. Gacesa, R. et al. Environmental factors shaping the gut microbiome in a Dutch population. *Nature* **604**, 732–739 (2022).
11. Derosa, L. et al. Gut bacteria composition drives primary resistance to cancer immunotherapy in renal cell carcinoma patients. *Eur. Urol.* **78**, 195 (2020).
12. Kim, C. G. et al. Prior antibiotic administration disrupts anti-PD-1 responses in advanced gastric cancer by altering the gut microbiome and systemic immune response. *Cell Rep. Med.* **4**, 101251 (2023).
13. Davar, D. et al. Fecal microbiota transplant overcomes resistance to anti-PD-1 therapy in melanoma patients. *Science* **371**, 595–602 (2021).
14. Baruch, E. N. et al. Fecal microbiota transplant promotes response in immunotherapy-refractory melanoma patients. *Science* **371**, 602–609 (2021).
15. Alves Costa Silva, C., Almonte, A. A. & Zitvogel, L. Oncobiomics: leveraging microbiome translational research in immuno-oncology for clinical-practice changes. *Biomolecules* **15**, 504 (2025).
16. Routy, B. et al. Fecal microbiota transplantation plus anti-PD-1 immunotherapy in advanced melanoma: a phase I trial. *Nat. Med.* **29**, 2121–2132 (2023).
17. Elkrief, A. et al. 1068P phase II trial of fecal microbiota transplantation (FMT) plus immune checkpoint inhibition (ICI) in advanced non-small cell lung cancer and cutaneous melanoma (FMT-LUMINATE). *Ann. Oncol.* **35**, S707 (2024).
18. Ciccarese, C. et al. LBA77 fecal microbiota transplantation (FMT) versus placebo in patients receiving pembrolizumab plus axitinib for metastatic renal cell carcinoma: preliminary results of the randomized phase II TACITO trial. *Ann. Oncol.* **35**, S1264 (2024).
19. Porcari, S. et al. Fecal microbiota transplantation to improve efficacy of immune checkpoint inhibitors in renal cell carcinoma (TACITO trial). *J. Clin. Oncol.* **40**, TPS407 (2022).
20. Dizman, N. et al. Nivolumab plus ipilimumab with or without live bacterial supplementation in metastatic renal cell carcinoma: a randomized phase 1 trial. *Nat. Med.* **28**, 704–712 (2022).
21. Ebrahimi, H. et al. Cabozantinib and nivolumab with or without live bacterial supplementation in metastatic renal cell carcinoma: a randomized phase 1 trial. *Nat. Med.* **30**, 2576–2585 (2024).
22. Routy, B. et al. Gut microbiome influences efficacy of PD-1-based immunotherapy against epithelial tumors. *Science* **359**, 91–97 (2018).
23. Pasolli, E., Truong, D. T., Malik, F., Waldron, L. & Segata, N. Machine learning meta-analysis of large metagenomic datasets: tools and biological insights. *PLoS Comput. Biol.* **12**, e1004977 (2016).
24. Derosa, L. et al. Custom scoring based on ecological topology of gut microbiota associated with cancer immunotherapy outcome. *Cell* **187**, 3373–3389 (2024).
25. Fidelle, M. et al. A microbiota-modulated checkpoint directs immunosuppressive intestinal T cells into cancers. *Science* **380**, eab02296 (2023).
26. Choueiri, T. K. et al. Avelumab+axitinib versus sunitinib as first-line treatment for patients with advanced renal cell carcinoma: final analysis of the phase III JAVELIN Renal 101 trial. *Ann. Oncol.* **36**, 387–392 (2025).
27. Choueiri, T. K. et al. Updated efficacy results from the JAVELIN Renal 101 trial: first-line avelumab plus axitinib versus sunitinib in patients with advanced renal cell carcinoma. *Ann. Oncol.* **31**, 1030 (2020).
28. Thiery-Vuillemin, A. et al. Randomized phase II study to assess the efficacy and tolerability of sunitinib by dose administration regimen in anti-angiogenic naïve patients with metastatic renal cell carcinoma (mRCC): final analysis of SURF study. *J. Clin. Oncol.* **40**, 344 (2022).
29. Albiges, L. et al. Safety and efficacy of nivolumab in metastatic renal cell carcinoma (mRCC): final analysis from the NIVOREN GETUG AFU 26 study. *J. Clin. Oncol.* **37**, 542 (2019).
30. Ketas, T. J. et al. Antibody responses to SARS-CoV-2 mRNA vaccines are detectable in saliva. *Pathog. Immun.* **6**, 116–134 (2021).
31. Stolarz-Skrzypek, K. Fatal and nonfatal outcomes, incidence of hypertension, and blood pressure changes in relation to urinary sodium excretion. *JAMA* **305**, 1777 (2011).
32. Birebent, R. et al. Surrogate markers of intestinal dysfunction associated with survival in advanced cancers. *Oncoimmunology* **14**, 2484880 (2025).
33. Bredon, M. et al. *Faecalibacterium prausnitzii* strain EXL01 boosts efficacy of immune checkpoint inhibitors. *Oncoimmunology* **13**, 2374954 (2024).
34. Gopalakrishnan, V. et al. Gut microbiome modulates response to anti-PD-1 immunotherapy in melanoma patients. *Science* **359**, 97–103 (2018).
35. Matson, V. et al. The commensal microbiome is associated with anti-PD-1 efficacy in metastatic melanoma patients. *Science* **359**, 104–108 (2018).
36. Chen, J. et al. Low-dose irradiation of the gut improves the efficacy of PD-L1 blockade in metastatic cancer patients. *Cancer Cell* **43**, 361–379 (2025).
37. Zitvogel, L. et al. Impact of the ONCOBIOME network in cancer microbiome research. *Nat. Med.* **31**, 1085–1098 (2025).
38. Piccinno, G. et al. Pooled analysis of 3,741 stool metagenomes from 18 cohorts for cross-stage and strain-level reproducible microbial biomarkers of colorectal cancer. *Nat. Med.* **31**, 2416–2429 (2025).
39. Marcos-Kovandzic, L. et al. Gut microbiota modulation through *Akkermansia* spp. supplementation increases CAR T-cell potency. *Cancer Discov.* **15**, 1905–1926 (2025).
40. Grant, A. J., Lalor, P. F., Hübscher, S. G., Briskin, M. & Adams, D. H. MAdCAM-1 expressed in chronic inflammatory liver disease supports mucosal lymphocyte adhesion to hepatic endothelium (MAdCAM-1 in chronic inflammatory liver disease). *Hepatology* **33**, 1065–1072 (2001).
41. Laurans, L. et al. An obesogenic diet increases atherosclerosis through promoting microbiota dysbiosis-induced gut lymphocyte trafficking into the periphery. *Cell Rep.* **42**, 113350 (2023).
42. Feliu, V. et al. Distant antimetastatic effect of enterotropic colon cancer-derived $\alpha 4\beta 7^+$ CD8 $^+$ T cells. *Sci. Immunol.* **8**, eadg8841 (2023).
43. Zitvogel, L., Fidelle, M. & Kroemer, G. Long-distance microbial mechanisms impacting cancer immunosurveillance. *Immunity* **57**, 2013–2029 (2024).
44. Derosa, L. et al. Intestinal *Akkermansia muciniphila* predicts clinical response to PD-1 blockade in patients with advanced non-small-cell lung cancer. *Nat. Med.* **28**, 315–324 (2022).

45. Belluomini, L. et al. 1172O *Akkermansia muciniphila*-based multi-omic profiling in advanced non-small cell lung cancer. *Ann. Oncol.* **35**, S762 (2024).
46. Goel, A. et al. Toward a health-associated core keystone index for the human gut microbiome. *Cell Rep.* **44**, 115378 (2025).
47. Ebrahimi, H. Effect of CBM588 in combination with cabozantinib plus nivolumab for patients (pts) with metastatic renal cell carcinoma (mRCC): a randomized clinical trial. *J. Clin. Oncol.* **41**, LBA104 (2023).
48. NIH. A phase 1/2 study of Oncobax®-AK administered in combination with immunotherapy to patients with advanced solid tumors. *ClinicalTrials.gov* <https://clinicaltrials.gov/study/NCT05865730> (2023).

Publisher's note Springer Nature remains neutral with regard to jurisdictional claims in published maps and institutional affiliations.

Open Access This article is licensed under a Creative Commons Attribution-NonCommercial-NoDerivatives 4.0 International License, which permits any non-commercial use, sharing, distribution and reproduction in any medium or format, as long as you give appropriate credit to the original author(s) and the source, provide a link to the Creative Commons licence, and indicate if you modified the licensed material. You do not have permission under this licence to share adapted material derived from this article or parts of it. The images or other third party material in this article are included in the article's Creative Commons licence, unless indicated otherwise in a credit line to the material. If material is not included in the article's Creative Commons licence and your intended use is not permitted by statutory regulation or exceeds the permitted use, you will need to obtain permission directly from the copyright holder. To view a copy of this licence, visit <http://creativecommons.org/licenses/by-nc-nd/4.0/>.

© The Author(s) 2026

¹Gustave Roussy Cancer Campus, ClinicObiome, Villejuif, France. ²Oncoclinicas & Co—Medica Scientia Innovation Research (MEDSIR), São Paulo, São Paulo, Brazil. ³Gonçalo Moniz Institute, Oswaldo Cruz Foundation (FIOCRUZ), Salvador, Bahia, Brazil. ⁴Dana-Farber Cancer Institute (DFCI), Boston, MA, USA. ⁵Yale University, New Haven, CT, USA. ⁶Department of Agricultural Sciences, University of Naples Federico II, Naples, Italy. ⁷Task Force on Microbiome Studies, University of Naples Federico II, Naples, Italy. ⁸Department of Computational, Cellular and Integrative Biology, University of Trento, Trento, Italy. ⁹Clinical Research and Innovation Department, Centre Léon Bérard, Lyon, France. ¹⁰Institut National de la Santé Et de la Recherche Médicale (INSERM) UMR 1015, Équipe Labelisée—Ligue Nationale Contre le Cancer, Villejuif, France. ¹¹Methodology and quality of life in oncology unit, Besançon University Hospital, Besançon, France. ¹²EFS, INSERM UMR1098 RIGHT, Marie et Louis Pasteur University, Besançon, France. ¹³Department of Urology, University Hospital Leipzig, Leipzig, Germany. ¹⁴Paris-Saclay University, Le Kremlin Bicêtre, France. ¹⁵Department of Medical Oncology, Gustave Roussy Cancer Campus, Villejuif, France. ¹⁶IHU PRISM National Precision Medicine Center in Oncology, Villejuif, France. ¹⁷Immunomonitoring laboratory, INSERM US 23/CNRS3655, Université Paris-Saclay, Gif-sur-Yvette, France. ¹⁸Immune Cell Enhancers (ICE) Unit, Clinical Research Platform, Gustave Roussy, Villejuif, France. ¹⁹Translational Research, UNICANCER, Paris, France. ²⁰Jean Minjoz University Hospital, Besançon, France. ²¹Department of Radiation Oncology, Weill Cornell Medicine, New York City, NY, USA. ²²Sandra and Edward Meyer Cancer Center, New York City, NY, USA. ²³Department of Medicine, Weill Cornell Medical College, New York City, NY, USA. ²⁴Research Unit Hypertension and Cardiovascular Epidemiology, KU Leuven Department of Cardiovascular Sciences, University of Leuven, Leuven, Belgium. ²⁵Harvard Medical School, Boston, MA, USA. ²⁶These authors contributed equally: Carolina Alves Costa Silva, Marc Machaalani, Renee Maria Saliby. ²⁷These authors jointly supervised this work: Laurence Zitvogel, Toni K. Choueiri, Laurence Albiges.  e-mail: laurence.zitvogel@gustaveroussy.fr

Methods

Study participant details

Participant data were obtained from the following four prospective clinical trials in RCC: JAVELIN Renal 101 (ClinicalTrials.gov registration: [NCT02684006](#)), GETUG-AFU26 NIVOREN (ClinicalTrials.gov registration: [NCT03013335](#)), SURF (ClinicalTrials.gov registration: [NCT02689167](#)) and ONCOBIOTICS (ClinicalTrials.gov registration: [NCT04567446](#)).

Clinical trials

JAVELIN Renal 101 is a multicenter, randomized, open-label, phase 3 clinical trial evaluating the efficacy and safety of avelumab plus axitinib versus sunitinib monotherapy in patients with previously untreated advanced RCC with a clear-cell component. A total of 886 adults were enrolled and randomized 1:1 to receive either avelumab (10 mg kg⁻¹ intravenously every 2 weeks) plus axitinib (5 mg orally twice daily) or sunitinib (50 mg orally once daily for 4 weeks in a 6-week cycle). For alignment within the study, a single cycle consisted of 6 weeks for both treatment arms. The trial design has been previously described, and results are reported per CONSORT guidelines^{26,49}. The coprimary endpoints were PFS and OS in patients with PD-L1-positive tumors^{27,49}. A key secondary endpoint was PFS in the overall population; other endpoints included objective response rate (ORR). Efficacy data reported here reflect the second interim analysis of the JAVELIN Renal 101 trial, with a data cut-off of January 2019. Blood samples were collected at screening and on multiple days within cycles 1, 2 and 3, before treatment. Available baseline and cycle 3 samples were used in this analysis. The collection included whole blood in dipotassium ethylenediaminetetraacetic acid and silica-coated tubes for plasma and serum separation, respectively. Sample availability varied based on patient consent, local regulations, sample pairing, volume constraints and site-level data reporting. The protocol has been previously published⁴⁹.

GETUG-AFU26 NIVOREN trial is a French, multicenter, prospective, phase 2 clinical trial evaluating the activity and safety of nivolumab in patients with metastatic ccRCC who had previously failed on or after an antiangiogenic regimen, as previously published^{29,50,51}. Participants received nivolumab at 3 mg kg⁻¹ every 2 weeks and underwent radiological assessment every 8–12 weeks. Treatment was continued until disease progression, unacceptable toxicity, withdrawal of consent or death. The primary endpoint was to assess the incidence of high-grade adverse events (grades 3–4 and 5, as per CTCAE v4.0)²⁹. Secondary endpoints included ORR, PFS, OS and exploration of candidate blood biomarkers associated with response and/or prognosis to treatment. Blood samples were collected before and on different visits after Nivolumab start. Available baseline, cycle 3, cycle 7 and progression visit samples were used in this analysis.

SURF trial is a French prospective, randomized, open-label phase 2b study that included patients with metastatic ccRCC treated with sunitinib at a standard 50 mg daily for 4 weeks, followed by a 2-week rest period (4/2)²⁸. Patients requiring a dose adjustment due to toxicity were randomized between the standard 4/2 schedule at a reduced dose of 37.5 mg daily and the experimental 2/1 schedule at 50 mg daily. The primary objective was to assess the median duration of sunitinib treatment in each group. Key secondary objectives included PFS, OS, time to randomization, ORR, safety, sunitinib dose intensity, health-related quality of life and the description of main drivers triggering randomization. An exploratory endpoint included the identification of blood biomarkers related to the activity and/or toxicity of sunitinib. Available baseline blood samples were used in this report. The protocol has been previously published⁵².

RCC ONCOBIOTICS is a multicentric study evaluating gut microbiota-related biomarkers associated with outcome in advanced RCC treated with ICI alone or in combination with TKI at Gustave Roussy, in France. The study followed standard care until disease progression, unacceptable toxicity or completion of 2 years of ICI treatment. Eligibility criteria and baseline data, including recent medications, are in the trial protocol

and recorded in electronic case report forms. Blood and stool samples were collected before and on different visits after treatment started.

The ONCOBIOME network dataset^{32,37} includes data from different cancer cohorts. Data from patients with lung cancer were obtained from the Lung ONCOBIOTICS study (ClinicalTrials.gov registration: [NCT04567446](#)), a multicenter trial conducted across 14 centers in France and Canada. This study assessed the effect of the microbiome on treatment outcomes in patients with advanced NSCLC receiving anti-PD-(L)1 therapies, either alone or with chemotherapy. Patients were followed under standard care until disease progression, unacceptable toxicity or completion of 2 years of ICI therapy. Eligibility criteria and baseline data, including recent medications, were recorded in trial protocols and electronic case report forms. Baseline stool and paired blood samples for sMAdCAM-1 analysis were included in the pooled analysis. Data from patients with colorectal cancer were from the AtezoTRIBE study (ClinicalTrials.gov registration: [NCT03721653](#))⁵³, a phase 2 trial enrolling 218 patients with unresectable stage IV colorectal cancer. Participants were randomized 2:1 to receive FOLFOXIRI plus bevacizumab with or without atezolizumab (anti-PD-L1). All patients were treatment-naïve at the time of initial stool collection. Paired baseline stool and blood samples for sMAdCAM-1 analysis were included in the pooled analysis. Data from patients with bladder cancer were sourced from the French cohort of the STRONG phase 3b trial (ClinicalTrials.gov registration: [NCT03084471](#))⁵⁴, in which patients who had progressed on chemotherapy received durvalumab (150 mg every 4 weeks until progression). Paired stool and blood samples for sMAdCAM-1 analysis were included in the pooled analysis.

The WELCOME (protocol IRB 20-04021831) trial was conducted at Weill Cornell Medicine and New York Presbyterian Hospital. The protocol is available at <https://research.weill.cornell.edu/NYPWelcomeStudy> (ref. 30).

FLEMENGHO received ethical approval from the Ethics Committee of the University of Leuven ([S6701](#)). The FLEMENGHO cohort represents a random population sample stratified by sex and age from a geographically defined area in northern Belgium³¹.

The reported clinical trials comply with all relevant ethical regulations on research involving human participants.

Ethical approval and consent to participate. The study design and conduct complied with all relevant regulations regarding the use of human study participants and were conducted in accordance with the Declaration of Helsinki and Good Clinical Practice guidelines. All participants provided written informed consent. Data were reported disaggregated for sex and gender. Consent has been obtained for reporting and sharing individual-level data. Data and sample collection adhered to regulatory, ethical requirements and ICH E6(R2) Good Clinical Practice guidelines.

Monitoring of circulating sMAdCAM-1 levels. sMAdCAM-1 was quantified in patients' plasma samples with Bio-Plex 200 Systems (Bio-Rad) and sMAdCAM-1 kit from R&D Systems (Human Luminex Discovery Assay LXSAHM) at Gustave Roussy or Dana-Farber Cancer Institute laboratory units.

Monitoring of cytokine levels. Cytokine and chemokine concentrations in patient serum were determined using two multiplexed panels that assayed 32 total analytes (Rules-Based Medicine), including brain-derived neurotrophic factor (BDNF), eotaxin-1, factor VII, granulocyte-macrophage colony-stimulating factor (GM-CSF), intercellular adhesion molecule-1 (ICAM-1), interferon-γ (IFNγ), IL-1α, IL-1β, IL-1 receptor antagonist (IL-1RA), IL-2, IL-3, IL-4, IL-5, IL-6, IL-7, IL-8, IL-10, IL-12 p40, IL-12 p70, IL-15, IL-17, IL-18, IL-23, macrophage inflammatory protein 1-α (MIP-1α), MIP-1β, matrix metalloproteinase 3 (MMP3), MMP9, MCP-1, stem cell factor (SCF), tumor necrosis factor (TNF), lymphotxin-α (LTα, formerly known as TNFβ) and VEGF, as previously described⁵⁵.

Stool samples collection. Stool samples were self-collected by the participants at home according to the International Human Microbiome Standards (IHMS)_SOP 004 (<https://human-microbiome.org/index.php?id=Sop&num=004>) within the ONCOBIOTICS, AtezoTRIBE and French cohort of the STRONG phase 3b trial study protocols. Immediately after the collection, samples were stored in a refrigerator (0–4 °C) until transportation. Upon arrival at the biobank of the recruitment center (within 24 h), samples were stored at –80 °C in plastic tubes. All samples were processed following the International Human Microbiome Standards (IHMS) guidelines (SOP 03 V1).

Statistical methods. Quantitative data are described by the number of patients with available data, the number of missing values, the mean, s.d., median, minimum and maximum values and the first and third quartile values (Q1–Q3). sMAdCAM-1 values were compared between groups using the Mann–Whitney or Kruskal–Wallis test. Spearman rank correlation analyses between MAdCAM-1 and each of IL-6 and IL-8 were performed to evaluate the relationship between MAdCAM-1 and these inflammatory cytokines. Categorical groups (sMAdCAM-1 high versus low, or the dynamic groups from cycle 1 to cycle 3) were compared between treatments using the chi-squared test. The dynamic values from cycle 1 to cycle 3 (Fig. 4a) were compared using the Wilcoxon signed-rank test. OS was defined as the time, expressed in months, from treatment initiation to the date of death or the last known follow-up. Patients alive at the last follow-up date were censored. PFS was defined as the time, expressed in months, from treatment initiation to the date of the first event (progression or death). Patients were censored at the last disease/tumor assessment. The optimal cut-off value was determined by Contal and O’Quigley’s approach for the OS outcome based on sMAdCAM-1 values at cycle 1 in the training cohort⁵⁶. The assumption of linearity was visually checked by the Martingale residual plots as well as the Restricted Cubic Spline plots (with five knots). The discrimination of the fitted model was assessed by time-dependent AUC at 18 months and integrated AUC index across all follow-up times (ranging 0–1, with higher numbers indicating better discrimination performance)⁵⁷. The 18-month time point was chosen based on the median follow-up of 18.9 months in this cohort. Kaplan–Meier curves and Cox proportional hazards models were used to compare PFS and OS across the sMAdCAM groups (high versus low at cycle 1, or the dynamic groups from cycle 1 to cycle 3). The analysis at cycle 3 was based on a landmark approach calculated from cycle 3 (3 months) for OS and PFS. Analyses were performed using SAS (v9.4; SAS Institute), R packages (‘rms’ for restricted cubic spline plot; ‘timeROC’ for time-dependent ROC) and SAS Macro for determining the optimal cut-off (<https://support.sas.com/resources/papers/proceedings/proceedings/sugi28/261-28.pdf>).

Metagenomics analysis. DNA was extracted from aliquots of the same stool samples used for metaproteomic analysis using the IHMS SOP 07 V2 H and sequenced on an Ion Proton sequencer (Thermo Fisher Scientific). The sequencing was performed at a single site (MetaGenoPolis). Reads were cleaned using Alien Trimmer (v.0.4.0) to (1) remove resilient sequencing adapters and (2) trim low-quality nucleotides at the 3' side using a quality cut-off of 20 and a length cut-off of 45 bp. Cleaned reads were subsequently filtered from human and other possible food contaminant DNA using the human genome (GRCh38-p13), with an identity score threshold of 95%. For each metagenome, we profiled the taxonomic composition with MetaPhlAn-4 (ref. 58). For α diversity, we computed the per-sample Richness and Shannon indexes⁵⁹ using the vegan R package⁶⁰. Differences between groups were assessed using the Wilcoxon–Mann–Whitney test. For β -diversity, we computed between-samples Bray–Curtis dissimilarities using the vegan R package⁶⁰. Differential abundance analysis on taxonomic profiles between groups was performed using the LDA effect size (LefSE) software. The longitudinal analysis was performed with a Wilcoxon signed-rank

test (testing only features present in at least ten samples in one of the groups). None of the associations presented adjusted P values with Benjamini–Hochberg correction lower than 0.2. In Fig. 5, microbial features have been subset as the ones presenting 50% prevalence in both tested groups and a raw P value <0.05 .

Reporting summary

Further information on research design is available in the Nature Portfolio Reporting Summary linked to this article.

Data availability

MetaPhlAn4 profiles and Luminex data for the cohorts included in this study are available via Figshare (<https://doi.org/10.6084/m9.figshare.30336373>). The remaining data will be available within the article, Supplementary Information or source data file. Source data are provided with this paper.

References

- Motzer, R. J. et al. Avelumab plus axitinib versus sunitinib for advanced renal-cell carcinoma. *N. Engl. J. Med.* **380**, 1103–1115 (2019).
- Flippot, R. et al. Safety and efficacy of nivolumab in brain metastases from renal cell carcinoma: results of the GETUG-AFU 26 NIVOREN multicenter phase II study. *J. Clin. Oncol.* **37**, 2008–2016 (2019).
- Carril-Auria, L. et al. Baseline circulating unswitched memory B cells and B-cell related soluble factors are associated with overall survival in patients with clear cell renal cell carcinoma treated with nivolumab within the NIVOREN GETUG-AFU 26 study. *J. Immunother. Cancer* **10**, e004885 (2022).
- Mouillet, G. et al. Open-label, randomized multicentre phase II study to assess the efficacy and tolerability of sunitinib by dose administration regimen (dose modification or dose interruptions) in patients with advanced or metastatic renal cell carcinoma: study protocol of the SURF trial. *Trials* **19**, 221 (2018).
- Antoniotti, C. et al. Upfront FOLFOXIRI plus bevacizumab with or without atezolizumab in the treatment of patients with metastatic colorectal cancer (AtezoTRIBE): a multicentre, open-label, randomised, controlled, phase 2 trial. *Lancet Oncol.* **23**, 876–887 (2022).
- Sonpavde, G. P. et al. Primary results of STRONG: an open-label, multicenter, phase 3b study of fixed-dose durvalumab monotherapy in previously treated patients with urinary tract carcinoma. *Eur. J. Cancer* **163**, 55–65 (2022).
- Choueiri, T. K. et al. Integrative analyses of tumor and peripheral biomarkers in the treatment of advanced renal cell carcinoma. *Cancer Discov.* **14**, 406–423 (2024).
- Contal, C. & O’Quigley, J. An application of changepoint methods in studying the effect of age on survival in breast cancer. *Comput. Stat. Data Anal.* **30**, 253–270 (1999).
- Uno, H., Cai, T., Tian, L. & Wei, L. J. Evaluating prediction rules for t -year survivors with censored regression models. *J. Am. Stat. Assoc.* **102**, 527–537 (2007).
- Blanco-Míguez, A. et al. Extending and improving metagenomic taxonomic profiling with uncharacterized species using MetaPhlAn 4. *Nat. Biotechnol.* **41**, 1633–1644 (2023).
- Shannon, C. E. A mathematical theory of communication. *Bell Syst. Tech. J.* **27**, 379–423 (1948).
- Oksanen, J. et al. vegan: community ecology package. R package version 2.5-2, <https://doi.org/10.32614/CRAN.package.vegan> (2018).

Acknowledgements

Patients, investigators and study teams on the clinical trials are included. We would like to express our sincere gratitude to Pfizer and

EMD Serono for providing samples and datasets from the JAVELIN Renal 101 (NCT02684006) clinical trial, to the Wyss Institute for allowing us to use their instrument and to Shanda Lightbown and Nina LoGrande for their technical assistance. T.K.C. is supported in part by the Dana-Farber/Harvard Cancer Center Kidney SPORE (2P50CA101942-16) and Program 5P30CA006516-56, the Kohlberg Chair at Harvard Medical School and the Trust Family, Michael Brigham, Pan Mass Challenge, Hinda and Arthur Marcus Fund and Loker Pinard Funds for Kidney Cancer Research at DFCI. L.Z. and L.D. are supported by the SEERAVE Foundation; the European Union's Horizon Europe research and innovation program under grant agreement 101095604 (project acronym, PREVALUNG-EU; project title, Personalized Lung Cancer Risk Assessment Leading to Stratified Interception); the European Union's Horizon 2020 research and innovation program under grant agreement 825410 (ONCOBIOME project); Institut National du Cancer (INCa); Agence Nationale de la Recherche (ANR) Ileobiome—19-CE15-0029-01; ANR RHU5 'ANR-21-5 RHUS-0017' ('IMMUNOLIFE'); MAdCAM INCA_16698; Ligue contre le Cancer; the LabEx Immuno-Oncology (ANR-18-IDEX-0001); la Direction Générale de l'Offre de Soins (DGOS); Université Paris-Saclay; PACRI network; Ligue contre le Cancer (équipes labellisées Program 'Equipe labellisée LIGUE' EL2016.LNCC (VT/PLP)); ANR—Projets blancs; ANR under the frame of E-Rare-2 the ERA-Net for Research on Rare Diseases; AMMICA US23/CNRS UMS3655; Association pour la Recherche sur le Cancer (ARC); Association 'Le Cancer du Sein Parlons-en!'; Cancéropôle Ile-de-France; Chancellerie des Universités de Paris (Legs Poix); Fondation pour la Recherche Médicale (FRM); a donation by Elior; European Research Area Network on Cardiovascular Diseases (ERA-CVD MINOTAUR); Gustave Roussy Odyssea; Fondation Carrefour; INCa; Inserm (HTE); Institut Universitaire de France; LeDucq Foundation; SIRIC Cancer Research and Personalized Medicine (CARPEM); and the ARC (projects MICROBIONT-PREDICT (2021) Made-IT (2023)). C.A.C.S., L.D. and L.Z. were supported by the European Union's Horizon 2020 research and innovation program under grant agreement 964590 (project acronym, IHMCSA; project title, International Human Microbiome Coordination and Support Action). L.D. is supported by AACR 2025 Career Development Award in Lung Cancer Research and Association Robert Debré pour la Recherche Médicale. N.S. was supported by the European Research Council (ERC-CoG microTOUCH-101045015), the European Union's Horizon 2020 program (ONCOBIOME-825410 project), the National Cancer Institute of the National Institutes of Health (1U01CA230551) and the Premio Internazionale Lombardia e Ricerca 2019. Patient plasma samples were provided by EMD Serono, the healthcare business of Merck KGaA, Darmstadt, Germany (CrossRef Funder ID 10.13039/100009945). The bladder cancer cohort from the IOPREDI ancillary study/STRONG study (NCT03084471) was funded by AstraZeneca. The funders had no role in study design, data collection and analysis, decision to publish or preparation of the manuscript.

Author contributions

C.A.C.S., L.D., L.Z. and L.A. designed the study. C.A.C.S., M.M., R.M.S., M.F., G.M.L., R.B., E.S., C.S., R.F., J.B.M., N.S., A.T.V., S.F., T.K., B.E., L.D., L.Z., T.K.C. and L.A. contributed to data acquisition and investigation. C.A.C.S., M.M., R.M.S., C.Z., W.X., E.P., G.P., C.D., A.M., D.V. and L.D. performed formal analysis and validation. L.Z., T.K.C. and L.A. supervised the study. C.A.C.S., M.M., R.M.S., C.Z., W.X., E.P., L.D., L.Z., T.K.C. and L.A. wrote the original draft of the manuscript. All authors reviewed, edited and approved the final manuscript.

Competing interests

C.A.C.S. reports speaker honoraria fees from Ipsen, AstraZeneca and Bristol Myers-Squibb. L.A. received advisory, consulting or honoraria fees (all paid to their institution) from AMGEN, Astellas, AstraZeneca, Bristol Myers-Squibb, Daiichi, EISAI, Ipsen, Janssen, Merck, MSD, Novartis, Pfizer, Roche, Telix and Xencor. L.A. also received travel and

accommodations expenses from Bristol-Myers Squibb, IPSEN, MSD and Pfizer. T.K.C. reports institutional and/or personal, paid and/or unpaid support for research, advisory boards, consultancy and/or honoraria in the past 5 years, ongoing or not, from Alkermes, Arcus Bio, AstraZeneca, Aravive, Aveo, Bayer, Bristol-Myers Squibb, Bicycle Therapeutics, Calithera, Caris, Circle Pharma, Deciphera Pharmaceuticals, Eisai, EMD Serono, Exelixis, GlaxoSmithKline, Gilead, HiberCell, IQVA, Infinity, Institut Servier, Ipsen, Jansen, Kanaph, Lilly, Merck, Nikang, Neomorph, Nuscan/PrecedeBio, Novartis, Oncohost, Pfizer, Roche, Sanofi/Aventis, Scholar Rock, Surface Oncology, Takeda, Tempest, Up-To-Date, CME and non-CME events (Mashup Media Peerview, OncLive, MJH, CCO and others), and Xencor, outside the submitted work. Institutional patents have been filed on molecular alterations and immunotherapy response/toxicity, rare genitourinary cancers and ctDNA/liquid biopsies. Equity holdings include Tempest, Pionyr, Osel, PrecedeBio, CureResponse, InnDura Therapeutics, Primum, Abalytics and Faron Pharma. Committee involvement includes NCCN, GU Steering Committee, ASCO (BOD 6/2024-), ESMO, ACCRU and KidneyCan. Medical writing and editorial assistance support may have been funded by communications companies in part. T.K.C. has no speaker's bureau activities. T.K.C. has mentored several non-US citizens on research projects with potential funding (in part) from non-US sources/Foreign Components. The institution (Dana-Farber Cancer Institute) may have received additional independent funding from drug companies or/and royalties potentially involved in research around the subject matter. T.K.C. is supported in part by the Dana-Farber/Harvard Cancer Center Kidney SPORE (2P50CA101942-16) and Program 5P30CA006516-56, the Kohlberg Chair at Harvard Medical School and the Trust Family, Michael Brigham, Pan Mass Challenge, Hinda and Arthur Marcus Fund and Loker Pinard Funds for Kidney Cancer Research at DFCI. A.T.V. has received payment to their institution linked to the SURF clinical trial from Pfizer; has received a research grant for their institution from Pfizer, Bayer and Ipsen; has received consulting fees, payment or honoraria for lectures, presentations, speakers' bureaus, manuscript writing or educational events and support for attending meetings and/or travel from Roche, MSD, JNJ, BMS, Astellas, Ipsen, AstraZeneca and Novartis; has participated on a data safety monitoring board or advisory board for DSMB (BIONIKK trial); has been a BMS employee since 2023 and has BMS stocks; and is a member of the steering committee of the French GETUG academic group. E.S. received research funding from Roche/Genentech and Oncohost. R.F. reports research funding from Bayer and honoraria fees from Astellas, Bayer, Johnson and Johnson, Ipsen, Eisai, Pfizer, MSD and Merck Serono. W.X. reports consulting or advisory roles with PCCTC. C.S. reports speaker honoraria and advisory board fees from Eisai. The other authors declare no competing interests.

Additional information

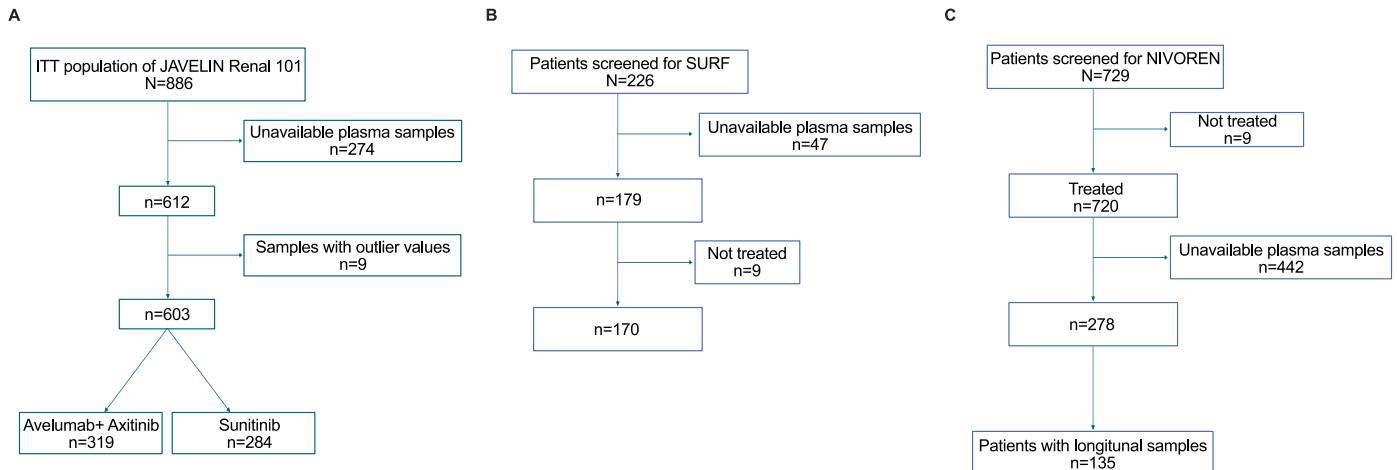
Extended data is available for this paper at <https://doi.org/10.1038/s41591-025-04067-x>.

Supplementary information The online version contains supplementary material available at <https://doi.org/10.1038/s41591-025-04067-x>.

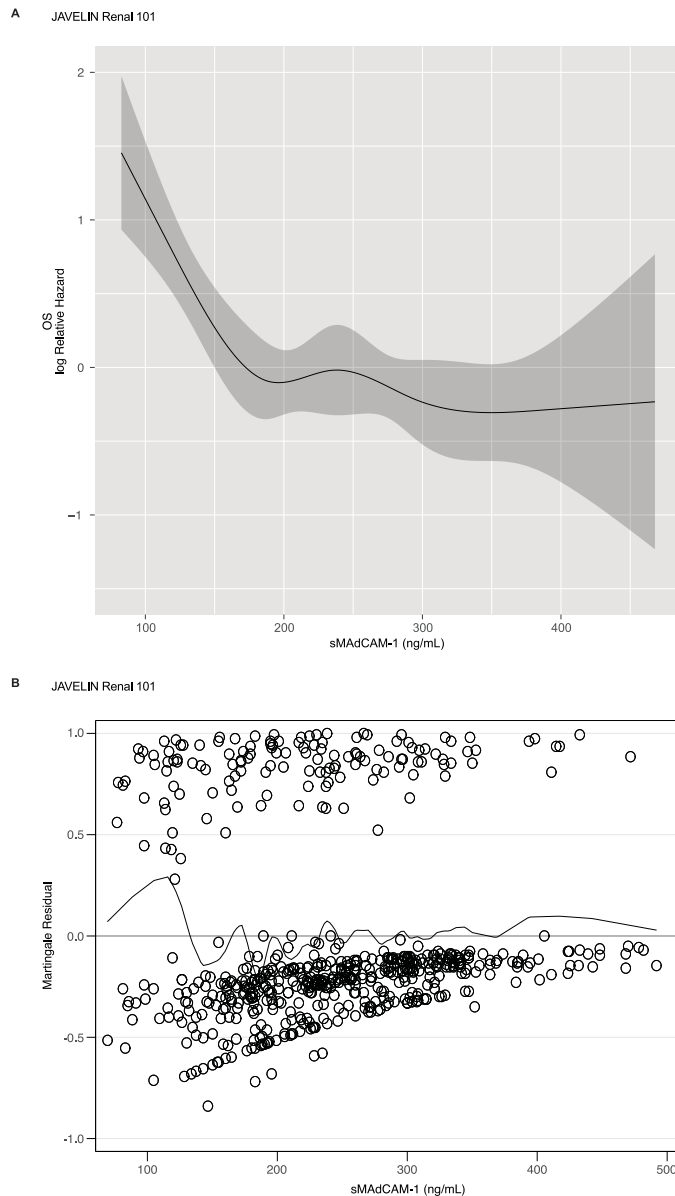
Correspondence and requests for materials should be addressed to Laurence Zitvogel.

Peer review information *Nature Medicine* thanks Jong-Hyeon Jeong, Brandon Manley and the other, anonymous, reviewer(s) for their contribution to the peer review of this work. Primary Handling Editor: Ulrike Harjes, in collaboration with the *Nature Medicine* team.

Reprints and permissions information is available at www.nature.com/reprints.

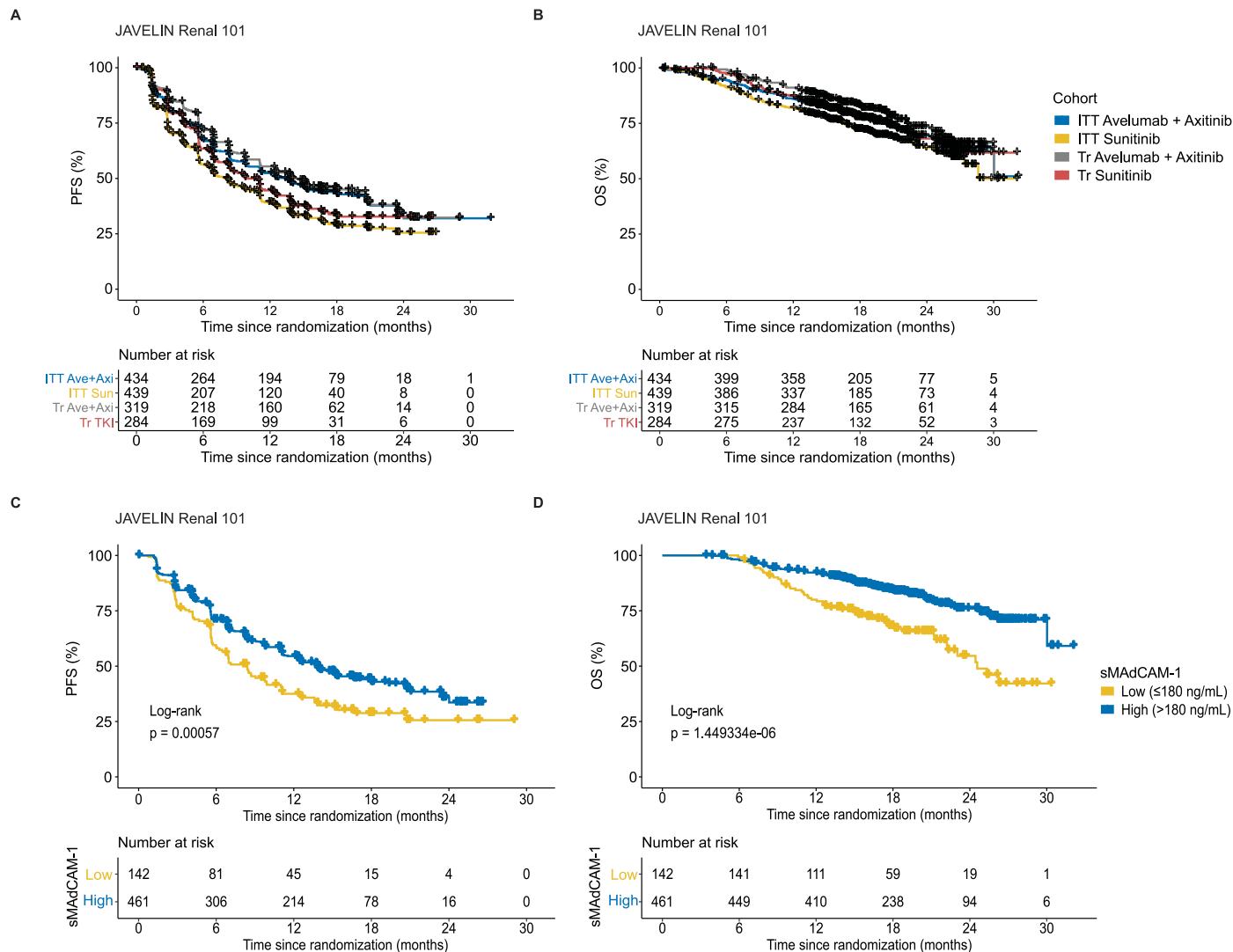


Extended Data Fig. 1 | Study participant flowcharts. Flowchart of study participants with renal cell carcinoma (RCC) in the JAVELIN Renal 101 (a), SURF (b) and NIVOREN (c) trials. Patients with unavailable plasma samples, outlier values, or who were not treated were excluded. ITT, intention-to-treat.



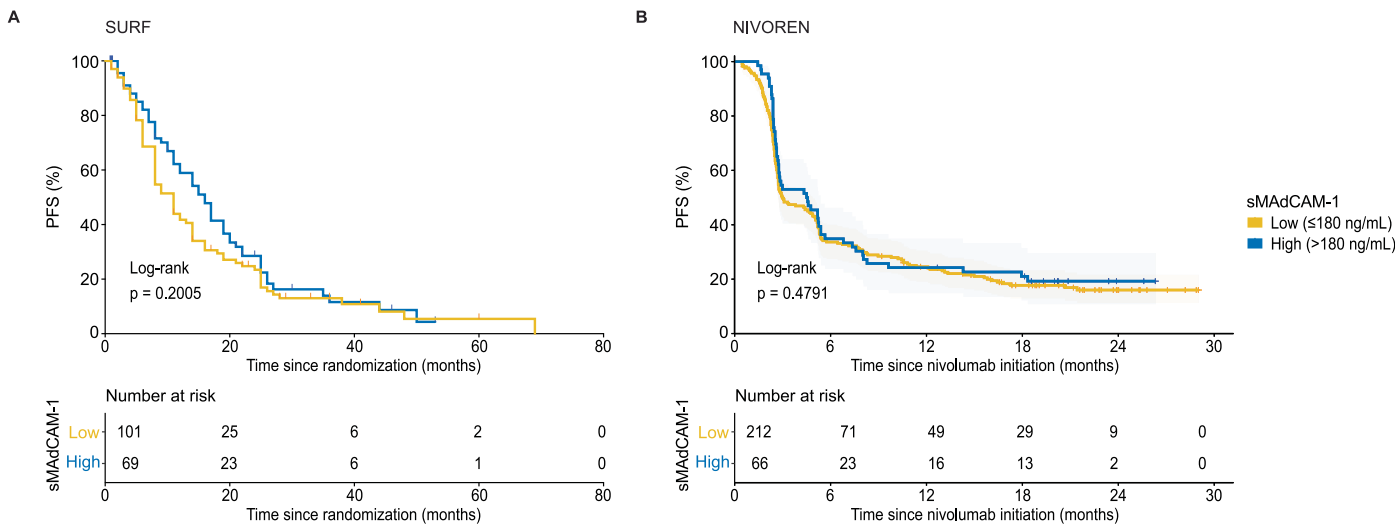
Extended Data Fig. 2 | Prognostic analysis of sMAdCAM-1. **a**, Restricted cubic spline plot showing the predicted risk score (log relative hazard, solid line) and 95% confidence interval (shaded area) for overall survival (OS) based on

the continuous sMAdCAM-1 values (ng/mL). Lower sMAdCAM-1 values were associated with a higher risk of death, and the curve tended to be flattened after values >180 ng/mL. **b**, Martingale residual plot.



Extended Data Fig. 3 | Soluble MAdCAM-1 linear distribution. a,b, Kaplan-Meier survival estimates of progression-free survival (PFS; **a**) and overall survival (OS; **b**) in patients from the JAVELIN Renal 101 trial showing both superposing curves for the intention-to-treat population and in the subset of patients analyzed in the biomarker ancillary study cohort from the trial, across both treatment arms. Risk tables indicate the number of patients at risk at each time

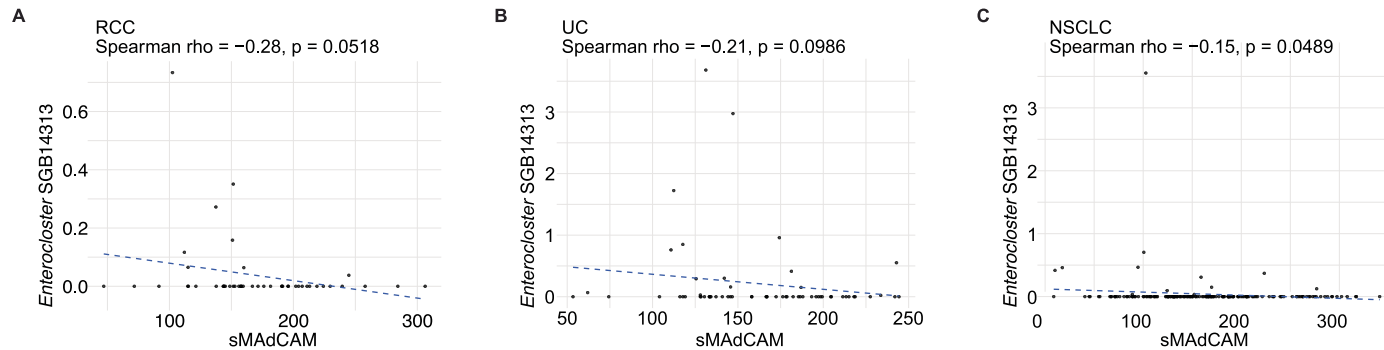
point. **c,d**, Kaplan-Meier survival estimates of PFS (**c**) and OS (**d**) stratified by sMAdCAM-1 concentrations in the JAVELIN Renal 101 trial. Patients were dichotomized using a threshold of 180 ng/mL into low (≤ 180 ng/mL) and high (> 180 ng/mL) sMAdCAM-1 groups. Survival differences were assessed using the log-rank test; P values are shown. Risk tables indicate the number of patients at risk at each time point.



Extended Data Fig. 4 | Levels of sMAdCAM-1 do not impact progression-free survival (PFS) in the SURF and NIVOREN trials (validation cohorts).

a,b, Kaplan–Meier survival estimates of PFS stratified by sMAdCAM-1 concentrations in the SURF (a) and NIVOREN (b) trials. Patients were

dichotomized using a threshold of 180 ng/mL into low (≤ 180 ng/mL) and high (> 180 ng/mL) sMAdCAM-1 groups. Survival differences were assessed using the log-rank test; P values are shown. Risk tables indicate the number of patients at risk at each time point.



Extended Data Fig. 5 | Levels of sMAdCAM-1 anticorrelate with *Enterocloster* SGB14313. **a–c**, Scatterplots showing the relationship between mucosal addressin cell adhesion molecule-1 (MAdCAM-1) concentrations in plasma samples and *Enterocloster* SGB14313 relative abundance in paired stool samples of patients with renal cell carcinoma (RCC, N = 55 paired samples;

a), urothelial cancer (UC, N = 61 paired samples; **b**) and non-small cell lung cancer (NSCLC, N = 188 paired samples; **c**). Each point represents an individual sample measurement. The dotted line represents the linear regression fit. Statistical comparisons between groups were performed using a two-sided Spearman test without adjustments for multiple comparisons; exact P values are shown.

Extended Data Table 1 | Multivariable analysis and model discrimination

Parameters'	PFS HR (95% CI)'			OS HR (95% CI)'		
Favorable +	Ref+		p-value+	Ref+		p-value+
Intermediate+	1.77 (1.31, 2.39)+		<0.001+	3.01 (1.60, 5.66)+		<0.001+
Poor+	2.88 (1.99, 4.17)+		<0.001+	7.91 (4.02, 15.56)+		<0.001+
MAdCAM-1 (high vs low)+	0.75 (0.59, 0.96)+		0.021+	0.59 (0.41, 0.85)+		0.004+
Models'	PFS'		'	OS'		'
	Integrated AUC+	AUC at 18 mo+	p-value (18 mo)+	Integrated AUC+	AUC at 18mo+	p-value (18 mo)'
Model1: + IMDC group only+	0.630+	0.607+	ref+	0.682+	0.684+	ref+
Model 5+ IMDC + MAdCAM-1 (high vs low)+	0.640+	0.615+	0.10+	0.699+	0.716+	0.01+

AUC: area under the curve; HR: hazard ratio; mo: months; OS: overall survival; PFS: progression-free survival; Ref: reference.+

Extended Data Table 2 | Multivariable Cox model for overall survival (OS) in the NIVOREN cohort (N=263)

Factor Label	Events/N	Hazard Ratio (95% CI)	P-value
ATB			0.1248
ATB non-users	107/226	1	
ATB users	23/37	1.44 (0.90-2.31)	
Madcam			0.0038
>180	19/63	1	
≤180	111/200	2.11 (1.27-3.49)	
Sex-at-birth			0.8560
Male	105/211	1	
Female	25/52	0.96 (0.61-1.51)	
Age (years)			0.0280
<70	85/184	1	
≥ 70	45/79	1.51 (1.05-2.19)	
IMDC			0.1910
Favorable	13/44	1	
Intermediate	75/151	1.67 (0.91-3.08)	
Poor	42/68	1.85 (0.94-3.63)	
Number of lines >2			0.6524
No	108/219	1	
Yes	22/44	0.90 (0.56-1.43)	
Brain metastasis			0.0004
No	112/237	1	
Yes	18/26	2.64 (1.55-4.50)	
Bone metastasis			0.0373
No	81/181	1	
Yes	49/82	1.48 (1.02-2.13)	
Liver metastasis			0.6545
Factor Label	Events/N	Hazard Ratio (95% CI)	P-value
No	93/191	1	
Yes	37/72	1.09 (0.74-1.62)	
Hypoalbuminemia			0.0103
No	71/169	1	
Yes	59/94	1.63 (1.12-2.36)	

Extended Data Table 3 | Cox proportional hazards models for longitudinal sMAdCAM-1 categories

	PFS		OS	
	HR (95% CI)	p-value	HR (95% CI)	p-value
High-High	0.53 (0.37, 0.76)	0.001	0.34 (0.23, 0.52)	<.001
Low-High	0.59 (0.36, 0.98)	0.041	0.64 (0.37, 1.12)	0.116
High-Low	0.52 (0.29, 0.92)	0.024	0.49 (0.26, 0.92)	0.026
Low-Low	ref	ref	ref	ref

Extended Data Table 4 | Linear discriminant analysis (LDA) effect size analysis by soluble MAdCAM-1 categories

Microbial species	p-value	Adjusted p-value	Effect size	Mean group1	Mean group2	Mean difference
<i>Clostridia</i> unclassified SGB4367	0,000448	0,121664	0,234691475	0,001980796	0,383000991	-0,381020195
<i>Lachnospiraceae bacterium</i> WCA3 601 WT 6H SGB4910	0,0281	0,385631429	0,146774024	0,122057788	0,396823243	-0,274765456
GGB3293 SGB4348	0,000677	0,124753125	0,227213725	0,145926903	0,37691018	-0,230983278
<i>Ruminococcaceae</i> unclassified SGB15234	0,00481	0,217709762	0,188495691	0,037997876	0,227612703	-0,189614827
<i>Collinsella aerofaciens</i> SGB14546	0,000768	0,124753125	0,224863865	0,040149027	0,212971081	-0,172822055
<i>Alistipes</i> sp An31A SGB2304	0,0231	0,373755932	0,152101568	0	0,135050541	-0,135050541
<i>Sutterella</i> SGB9281	0,0232	0,373755932	0,151878371	0,022569292	0,153784865	-0,131215573
<i>Bacilli</i> unclassified SGB6478	0,0156	0,323574468	0,161775892	0,001076283	0,107349459	-0,106273176
GGB1681 SGB2313	0,0126	0,30178375	0,166994305	0	0,103543423	-0,103543423
GGB9633 SGB15091	0,0198	0,355092453	0,155846344	0,074082035	0,172250901	-0,098168866
GGB9694 SGB15203	0,00105	0,124753125	0,219139092	0,002228142	0,095337477	-0,093109336
<i>Candidatus Cibiobacter qucibialis</i> SGB15286	0,0039	0,203458378	0,192911779	0,321246726	0,413197658	-0,091950932
GGB9633 SGB15090	0,0453	0,429109223	0,13391348	0,054128142	0,143807297	-0,089679156
GGB9712 SGB15244	0,0181	0,340369524	0,157959124	0,024920265	0,108919369	-0,083999104
<i>Bacteroides congonensis</i> SGB1878	0,0232	0,373755932	0,151878371	0,002440354	0,080929369	-0,078489015
<i>Desulfovibrio piger</i> SGB15465	0,0114	0,295425676	0,16922334	0,037779381	0,005026937	0,032752444
GGB9708 SGB15233	0,0321	0,393690968	0,143271198	0,123217434	0,089661982	0,033555452
<i>Lawsonibacter asaccharolyticus</i> SGB15154	0,00992	0,285726061	0,172369198	0,135863186	0,101724685	0,034138501
<i>Clostridium</i> SGB4909	0,0246	0,3756376	0,150264998	0,090066814	0,045930721	0,044136093
GGB33512 SGB15203	0,0445	0,429109223	0,134376587	0,083965044	0,034544955	0,049420089
GGB4745 SGB6571	0,0118	0,299090667	0,168317427	0,065199912	0,006625405	0,058574506
<i>Enterocloster</i> SGB14313	0,00525	0,2231774	0,186625649	0,069299646	0,006125856	0,06317379
<i>Vescimonas coprocola</i> SGB15089	0,000986	0,124753125	0,220204762	0,120462655	0,046075766	0,074386889
<i>Citrobacter</i> SGB1895	0,0465	0,429109223	0,133335967	0,117512301	0	0,117512301
GGB47687 SGB2286	0,0486	0,437860664	0,131852445	0,162797876	0,04482018	0,117977696
GGB79630 SGB13983	0,025	0,375813077	0,14988184	0,134390885	0,009000631	0,125390254
GGB51647 SGB4348	0,00767	0,275106981	0,178229022	0,308966195	0,177422162	0,131544033
GGB1680 SGB2312	0,0485	0,437860664	0,131959155	0,183816106	0,037314595	0,146501512
GGB1681 SGB2313	0,0126	0,30178375	0,166994305	0	0,103543423	-0,103543423
<i>Lachnospira pectinoschiza</i> SGB5075	0,046	0,429109223	0,133368821	0,738403451	0,358374054	0,380029397

Reporting Summary

Nature Portfolio wishes to improve the reproducibility of the work that we publish. This form provides structure for consistency and transparency in reporting. For further information on Nature Portfolio policies, see our [Editorial Policies](#) and the [Editorial Policy Checklist](#).

Statistics

For all statistical analyses, confirm that the following items are present in the figure legend, table legend, main text, or Methods section.

n/a Confirmed

- The exact sample size (n) for each experimental group/condition, given as a discrete number and unit of measurement
- A statement on whether measurements were taken from distinct samples or whether the same sample was measured repeatedly
- The statistical test(s) used AND whether they are one- or two-sided
Only common tests should be described solely by name; describe more complex techniques in the Methods section.
- A description of all covariates tested
- A description of any assumptions or corrections, such as tests of normality and adjustment for multiple comparisons
- A full description of the statistical parameters including central tendency (e.g. means) or other basic estimates (e.g. regression coefficient) AND variation (e.g. standard deviation) or associated estimates of uncertainty (e.g. confidence intervals)
- For null hypothesis testing, the test statistic (e.g. F , t , r) with confidence intervals, effect sizes, degrees of freedom and P value noted
Give P values as exact values whenever suitable.
- For Bayesian analysis, information on the choice of priors and Markov chain Monte Carlo settings
- For hierarchical and complex designs, identification of the appropriate level for tests and full reporting of outcomes
- Estimates of effect sizes (e.g. Cohen's d , Pearson's r), indicating how they were calculated

Our web collection on [statistics for biologists](#) contains articles on many of the points above.

Software and code

Policy information about [availability of computer code](#)

Data collection

Study participant details. Participant data were obtained from four prospective clinical trials in RCC: JAVELIN Renal 101 (ClinicalTrials.gov identifier: NCT02684006), GETUG-AFU 26 NIVOREN (ClinicalTrials.gov identifier: NCT03013335), SURF (ClinicalTrials.gov identifier: NCT02689167), and ONCOBIOTICS (ClinicalTrials.gov identifier: NCT04567446).

Clinical trials

JAVELIN Renal 101 is a multicenter, randomized, open-label, phase III clinical trial evaluating the efficacy and safety of avelumab plus axitinib versus sunitinib monotherapy in patients with previously untreated advanced RCC with a clear-cell component. A total of 886 adults were enrolled and randomized 1:1 to receive either avelumab (10 mg/kg IV every 2 weeks) plus axitinib (5 mg orally twice daily) or sunitinib (50 mg orally once daily for 4 weeks in a 6-week cycle). For alignment within the study, a single cycle consisted of 6 weeks for both treatment arms. The trial design has been previously described, and results are reported per CONSORT guidelines 1,2. The co-primary endpoints were progression-free survival (PFS) and overall survival (OS) in patients with PD-L1-positive tumors 1,3. A key secondary endpoint was PFS in the overall population; other endpoints included objective response rate (ORR). Efficacy data reported here reflect the second interim analysis of the JAVELIN Renal 101 trial, with a data cutoff of January 2019. Blood samples were collected at screening and on multiple days within cycles 1, 2, and 3, prior to treatment. Available baseline and cycle 3 samples were used in this analysis. Collection included whole blood in dipotassium ethylenediaminetetraacetic acid (K₂EDTA) and silica-coated tubes for plasma and serum separation, respectively. Sample availability varied based on patient consent, local regulations, sample pairing, volume constraints, and site-level data reporting. The protocol has been previously published 1.

GETUG-AFU 26 NIVOREN trial is a French, multicenter, prospective, phase II clinical trial evaluating the activity and safety of nivolumab in patients with metastatic ccRCC who had previously failed on or after an anti-angiogenic regimen, as previously published 4–6. Participants received nivolumab at 3 mg/kg every two weeks and underwent radiological assessment every 8–12 weeks. Treatment was continued until

disease progression, unacceptable toxicity, withdrawal of consent, or death. The primary endpoint was to assess the incidence of high-grade adverse events (Grades 3–4 and Grade 5, as per CTCAE v4.0) 4. Secondary endpoints included ORR, PFS, OS, and exploration of candidate blood biomarkers associated with response and/or prognosis to treatment. Blood samples were collected before and on different visits after Nivolumab start. Available baseline, cycle 3, cycle 7 and progression visit samples were used in this analysis.

SURF trial is a French prospective, randomized, open-label phase IIb study that included patients with metastatic ccRCC treated with sunitinib at a standard 50 mg daily for 4 weeks, followed by a 2-weeks rest period (4/2) 7. Patients requiring a dose adjustment due to toxicity were randomized between the standard 4/2 schedule at a reduced dose of 37.5 mg daily and the experimental 2/1 schedule at 50 mg daily. The primary objective was to assess the median duration of sunitinib treatment in each group. Key secondary objectives included PFS, OS, time to randomization, ORR, safety, sunitinib dose intensity, health-related quality of life, and the description of main drivers triggering randomization. An exploratory endpoint included the identification of blood biomarkers related to the activity and/or toxicity of sunitinib. Available baseline blood samples were used in this report. The protocol has been previously published 8.

RCC ONCOBIOTICS is a multicentric study evaluating gut microbiota related biomarkers associated with outcome in advanced RCC treated with ICI alone or in combination with TKI at Gustave Roussy, in France. The study followed standard care until disease progression, unacceptable toxicity, or completion of 2 years of ICI treatment. Eligibility criteria and baseline data, including recent medications, are in the trial protocol and recorded in electronic case report forms. Blood and stool samples were collected before and on different visits after treatment start.

The ONCOBIOME network dataset 9,10 includes data from different cancer cohorts. Data from patients with lung cancer were obtained from the Lung ONCOBIOTICS study (ClinicalTrials.gov identifier: NCT04567446), a multicenter trial conducted across 14 centers in France and Canada. This study assessed the impact of the microbiome on treatment outcomes in patients with advanced non–small cell lung cancer (NSCLC) receiving anti–PD-(L)1 therapies, either alone or with chemotherapy. Patients were followed under standard care until disease progression, unacceptable toxicity, or completion of two years of ICI therapy. Eligibility criteria and baseline data, including recent medications, were recorded in trial protocols and electronic case report forms. Baseline stool and paired blood samples for sMAdCAM-1 analysis were included in the pooled analysis. Data from patients with colorectal cancer were from the AtezoTRIBE study (ClinicalTrials.gov identifier: NCT03721653) 11, a phase II trial enrolling 218 patients with unresectable stage IV colorectal cancer. Participants were randomized 2:1 to receive FOLFOXIRI plus bevacizumab with or without atezolizumab (anti–PD-L1). All patients were treatment-naïve at the time of initial stool collection. Paired baseline stool and blood samples for sMAdCAM-1 analysis were included in the pooled analysis. Data from patients with bladder cancer were sourced from the French cohort of the STRONG phase IIIb trial (ClinicalTrials.gov identifier: NCT03084471) 12, in which patients who had progressed on chemotherapy received durvalumab (150 mg every 4 weeks until progression). Paired stool and blood samples for sMAdCAM-1 analysis were included in the pooled analysis.

The WELCOME (WEll CORnell Medicine Employees) (protocol number IRB# 20-04021831) trial was conducted at Weill Cornell Medicine (WCM) and New York Presbyterian Hospital (NYP). The protocol is available at <https://research.weill.cornell.edu/NYPWelcomeStudy> 13.

The Flemish study on Environment, Genes and Health Outcomes (FLEMENGHO) received ethical approval from the Ethics Committee of the University of Leuven (S67011). The FLEMENGHO cohort represents a random population sample stratified by sex and age from a geographically defined area in northern Belgium 14.

The reported clinical trials comply with all relevant ethical regulations on Research Involving Human Subjects.

Ethics approval and consent to participate. The study design and conduct complied with all relevant regulations regarding the use of human study participants and were conducted in accordance with the Declaration of Helsinki and Good Clinical Practice (GCP) guidelines. All participants provided written informed consent. Data was reported disaggregated for sex and gender. Consent has been obtained for reporting and sharing individual-level data. Data and sample collection adhered to regulatory, ethical requirements and ICH E6(R2) GCP guidelines.

Stool samples collection. Stool samples were self-collected by the participants at home according to the IHMS_SOP 004 (<https://human-microbiome.org/index.php?id=Sop&num=004>) within the ONCOBIOTICS, AtezoTRIBE and French cohort of the STRONG phase IIIb trial study protocols. Immediately after the collection, they were stored at -20°C and transported on dry ice. Upon arriving at the biobank of the recruitment center (between 4 and 24 h later), they were stored at -80°C in plastic tubes. Two aliquots of the same sample were used for metaproteomic and metagenomic analyses. All the samples were processed according to International Human Microbiome Standards (IHMS) guidelines (SOP 03 V1).

Data analysis

Statistical methods. Quantitative data are described by the number of patients with available data, the number of missing values, the mean, standard deviation, median, minimum and maximum values, and the 1st and 3rd quartile values (Q1–Q3). sMAdCAM-1 values were compared between groups using the Mann–Whitney or Kruskal–Wallis test. Spearman rank correlation analyses between MAdCAM-1 and each of interleukin-6 (IL-6) and interleukin-8 (IL-8) were performed to evaluate the relationship between MAdCAM-1 and these inflammatory cytokines. Categorical groups (sMAdCAM-1 high vs low, or the dynamic groups from Cycle 1 to Cycle 3) were compared between treatments using the Chi-square test. The dynamic values from Cycle 1 to Cycle 3 (Fig. 4A) were compared Wilcoxon signed-rank test. OS was defined as the time, expressed in months, from treatment initiation to the date of death or the last known follow-up. Patients alive at the last follow-up date were censored. PFS was defined as the time, expressed in months, from treatment initiation to the date of the first event (progression or death). Patients were censored at last disease/tumor assessment. The optimal cutoff value was determined by the Contal and O’Quigley’s approach for the OS outcome based on sMAdCAM-1 values at Cycle 1 in the training cohort 16. The assumption of linearity was visually checked by the Martingale residual plots as well as Restricted Cubic Spline plots (with 5 knots). The discrimination of the fitted model was assessed by time-dependent AUC at 18 months and Integrated AUC index across all follow up times (ranging 0–1, with higher numbers indicating better discrimination performance) 17. The 18-month timepoint was chosen based on the median follow-up of 18.9 months in this cohort. Kaplan–Meier curves and Cox proportional hazards models were used to compare PFS and OS across the sMAdCAM groups (high vs low at Cycle 1, or the dynamic groups from Cycle 1 to Cycle 3). The analysis at Cycle 3 was based on a landmark approach calculated from Cycle 3 (3-months) for OS and PFS. Analyses were performed using SAS 9.4 (SAS Institute Inc. Cary, NC), R packages (“rms” for Restricted Cubic Spline plot; “timeROC” for time-dependent ROC), and SAS Macro for determining the optimal cutoff (<https://support.sas.com/resources/papers/proceedings/proceedings/sugi28/261-28.pdf>).

Metagenomics analysis. DNA was extracted from an aliquot of the same stool samples used for metaproteomic analysis using the IHMS SOP 07 V2 H and sequenced with an Ion proton sequencer (Thermo Fisher Scientific). The sequencing was performed at a single site (MetaGenoPolis). Reads were cleaned using Alien Trimmer (version 0.4.0) to (1) remove resilient sequencing adapters and (2) trim low-quality nucleotides at the 3' side using a quality cutoff of 20 and a length cutoff of 45 bp. Cleaned reads were subsequently filtered from human and other possible food contaminant DNA using human genome (GRCh38-p13), with an identity score threshold of 95%. For each metagenome we profiled the taxonomic composition with MetaPhiAn-4 18. For alpha diversity, we computed the per-sample Richness and Shannon indexes 19 using the vegan R package 20. Differences between groups were assessed using the Wilcoxon–Mann–Whitney test. For beta-diversity, we computed the between-samples Bray–Curtis dissimilarities using the implementation available in the Vegan R package 20. Differential abundance analysis on taxonomic profiles between groups were performed using the LefSE software. The longitudinal analysis was performed with a Wilcoxon signed-rank test (testing only features present in at least 10 samples in one of the groups). None of the associations

presented adjusted p-values with Benjamini-Hochberg correction lower than 0.2. In figures, microbial features have been subset as the ones presenting 50% prevalence in both tested groups and raw p-value < 0.05.

For manuscripts utilizing custom algorithms or software that are central to the research but not yet described in published literature, software must be made available to editors and reviewers. We strongly encourage code deposition in a community repository (e.g. GitHub). See the Nature Portfolio [guidelines for submitting code & software](#) for further information.

Data

Policy information about [availability of data](#)

All manuscripts must include a [data availability statement](#). This statement should provide the following information, where applicable:

- Accession codes, unique identifiers, or web links for publicly available datasets
- A description of any restrictions on data availability
- For clinical datasets or third party data, please ensure that the statement adheres to our [policy](#)

MetaPhlAn4 profiles and Luminex data for the cohorts included in this study are available via Figshare. The remaining data will be available within the Article, Supplementary Information or Source Data file.

Research involving human participants, their data, or biological material

Policy information about studies with [human participants or human data](#). See also policy information about [sex, gender \(identity/presentation\), and sexual orientation](#) and [race, ethnicity and racism](#).

Reporting on sex and gender

Sex and/or gender were not considered in the studies design. Sex-at-birth (assigned) was collected per protocol detailed in previous publications. The sex, number and age of participants are described in Table 1.

Reporting on race, ethnicity, or other socially relevant groupings

Not reported.

Population characteristics

Relevant patient characteristics are described in Table 1 and previous published articles.

Recruitment

Participant data were obtained from four prospective clinical trials in RCC: JAVELIN Renal 101 (NCT02684006), GETUG-AFU 26 NIVOREN (NCT03013335), SURF (NCT02689167), and ONCOBIOTICS (NCT04567446). The study design and sample size have been reported previously. In this paper, all patients with available stool and serum samples submitted to translational research were included.

Ethics oversight

Ethics approval and consent to participate. The study design and conduct complied with all relevant regulations regarding the use of human study participants and were conducted was conducted in accordance with the Declaration of Helsinki and Good Clinical Practice (GCP) guidelines. All participants provided written informed consent. Consent to publish clinical information potentially identifying individuals was obtained (age and sex). Data and sample collection adhered to regulatory, ethical requirements and ICH E6(R2) GCP guidelines.

Note that full information on the approval of the study protocol must also be provided in the manuscript.

Field-specific reporting

Please select the one below that is the best fit for your research. If you are not sure, read the appropriate sections before making your selection.

Life sciences Behavioural & social sciences Ecological, evolutionary & environmental sciences

For a reference copy of the document with all sections, see nature.com/documents/nr-reporting-summary-flat.pdf

Life sciences study design

All studies must disclose on these points even when the disclosure is negative.

Sample size

Participant data were obtained from four prospective clinical trials in RCC: JAVELIN Renal 101 (NCT02684006), GETUG-AFU 26 NIVOREN (NCT03013335), SURF (NCT02689167), and ONCOBIOTICS (NCT04567446). The study design and sample size have been reported previously. In this paper, all patients with available stool and serum samples collected for translational research purposes were included.

Data exclusions

We only excluded samples that did not pass quality control check.

Replication

Direct replication via a separate cohort was not feasible due to the limited availability of samples from this specific clinical trial population. However, the robustness of the Luminex platform is well-established, and the findings are internally validated through their correlation with clinical outcomes.

Randomization

We confirm that for the biomarker analyses, group allocation was not random but was defined by data-driven biomarker cut-offs (e.g., high

Randomization

vs. low sMAdCAM-1). To account for potential confounding factors arising from this non-randomized allocation, we performed multivariable analyses adjusting for key clinical covariates such as IMDC risk group, age, and antibiotics use.

Blinding

Participant data were obtained from four prospective clinical trials in RCC: JAVELIN Renal 101 (NCT02684006), GETUG-AFU 26 NIVOREN (NCT03013335), SURF (NCT02689167), and ONCOBIOTICS (NCT04567446). We confirm that for the biomarker analyses, blinding was not relevant as the experimental groups were defined by data-driven biomarker cut-offs (e.g., high vs. low sMAdCAM-1). The group allocation itself was determined by the outcome of the measurement, making blinding of the investigators during data collection and analysis not applicable to this specific study design.

Reporting for specific materials, systems and methods

We require information from authors about some types of materials, experimental systems and methods used in many studies. Here, indicate whether each material, system or method listed is relevant to your study. If you are not sure if a list item applies to your research, read the appropriate section before selecting a response.

Materials & experimental systems

n/a	Involved in the study <input checked="" type="checkbox"/> Antibodies <input checked="" type="checkbox"/> Eukaryotic cell lines <input checked="" type="checkbox"/> Palaeontology and archaeology <input checked="" type="checkbox"/> Animals and other organisms <input type="checkbox"/> Clinical data <input checked="" type="checkbox"/> Dual use research of concern <input checked="" type="checkbox"/> Plants
-----	--

Methods

n/a	Involved in the study <input checked="" type="checkbox"/> ChIP-seq <input checked="" type="checkbox"/> Flow cytometry <input checked="" type="checkbox"/> MRI-based neuroimaging
-----	---

Clinical data

Policy information about [clinical studies](#)

All manuscripts should comply with the ICMJE [guidelines for publication of clinical research](#) and a completed [CONSORT checklist](#) must be included with all submissions.

Clinical trial registration

Participant data were obtained from four prospective clinical trials in RCC: JAVELIN Renal 101 (ClinicalTrials.gov identifier: NCT02684006), GETUG-AFU 26 NIVOREN (ClinicalTrials.gov identifier: NCT03013335), SURF (ClinicalTrials.gov identifier: NCT02689167), and ONCOBIOTICS (ClinicalTrials.gov identifier: NCT04567446).

Study protocol

Clinical trials
JAVELIN Renal 101 is a multicenter, randomized, open-label, phase III clinical trial evaluating the efficacy and safety of avelumab plus axitinib versus sunitinib monotherapy in patients with previously untreated advanced RCC with a clear-cell component. A total of 886 adults were enrolled and randomized 1:1 to receive either avelumab (10 mg/kg IV every 2 weeks) plus axitinib (5 mg orally twice daily) or sunitinib (50 mg orally once daily for 4 weeks in a 6-week cycle). For alignment within the study, a single cycle consisted of 6 weeks for both treatment arms. The trial design has been previously described, and results are reported per CONSORT guidelines 1,2. The co-primary endpoints were progression-free survival (PFS) and overall survival (OS) in patients with PD-L1-positive tumors 1,3. A key secondary endpoint was PFS in the overall population; other endpoints included objective response rate (ORR). Efficacy data reported here reflect the second interim analysis of the JAVELIN Renal 101 trial, with a data cutoff of January 2019. Blood samples were collected at screening and on multiple days within cycles 1, 2, and 3, prior to treatment. Available baseline and cycle 3 samples were used in this analysis. Collection included whole blood in dipotassium ethylenediaminetetraacetic acid (K₂EDTA) and silica-coated tubes for plasma and serum separation, respectively. Sample availability varied based on patient consent, local regulations, sample pairing, volume constraints, and site-level data reporting. The protocol has been previously published 1.

GETUG-AFU 26 NIVOREN trial is a French, multicenter, prospective, phase II clinical trial evaluating the activity and safety of nivolumab in patients with metastatic ccRCC who had previously failed on or after an anti-angiogenic regimen, as previously published 4–6. Participants received nivolumab at 3 mg/kg every two weeks and underwent radiological assessment every 8–12 weeks. Treatment was continued until disease progression, unacceptable toxicity, withdrawal of consent, or death. The primary endpoint was to assess the incidence of high-grade adverse events (Grades 3–4 and Grade 5, as per CTCAE v4.0) 4. Secondary endpoints included ORR, PFS, OS, and exploration of candidate blood biomarkers associated with response and/or prognosis to treatment. Blood samples were collected before and on different visits after Nivolumab start. Available baseline, cycle 3, cycle 7 and progression visit samples were used in this analysis.

SURF trial is a French prospective, randomized, open-label phase IIb study that included patients with metastatic ccRCC treated with sunitinib at a standard 50 mg daily for 4 weeks, followed by a 2-weeks rest period (4/2) 7. Patients requiring a dose adjustment due to toxicity were randomized between the standard 4/2 schedule at a reduced dose of 37.5 mg daily and the experimental 2/1 schedule at 50 mg daily. The primary objective was to assess the median duration of sunitinib treatment in each group. Key secondary objectives included PFS, OS, time to randomization, ORR, safety, sunitinib dose intensity, health-related quality of life, and the description of main drivers triggering randomization. An exploratory endpoint included the identification of blood biomarkers related to the activity and/or toxicity of sunitinib. Available baseline blood samples were used in this report. The protocol has been previously published 8.

RCC ONCOBIOTICS is a multicentric study evaluating gut microbiota related biomarkers associated with outcome in advanced RCC treated with ICI alone or in combination with TKI at Gustave Roussy, in France. The study followed standard care until disease progression, unacceptable toxicity, or completion of 2 years of ICI treatment. Eligibility criteria and baseline data, including recent medications, are in the trial protocol and recorded in electronic case report forms. Blood and stool samples were collected before

and on different visits after treatment start.

The ONCOBIOME network dataset 9,10 includes data from different cancer cohorts. Data from patients with lung cancer were obtained from the Lung ONCOBIOTICS study (ClinicalTrials.gov identifier: NCT04567446), a multicenter trial conducted across 14 centers in France and Canada. This study assessed the impact of the microbiome on treatment outcomes in patients with advanced non–small cell lung cancer (NSCLC) receiving anti–PD-(L)1 therapies, either alone or with chemotherapy. Patients were followed under standard care until disease progression, unacceptable toxicity, or completion of two years of ICI therapy. Eligibility criteria and baseline data, including recent medications, were recorded in trial protocols and electronic case report forms. Baseline stool and paired blood samples for sMAdCAM-1 analysis were included in the pooled analysis. Data from patients with colorectal cancer were from the AtezoTRIBE study (ClinicalTrials.gov identifier: NCT03721653) 11, a phase II trial enrolling 218 patients with unresectable stage IV colorectal cancer. Participants were randomized 2:1 to receive FOLFOXIRI plus bevacizumab with or without atezolizumab (anti–PD-L1). All patients were treatment-naïve at the time of initial stool collection. Paired baseline stool and blood samples for sMAdCAM-1 analysis were included in the pooled analysis. Data from patients with bladder cancer were sourced from the French cohort of the STRONG phase IIb trial (ClinicalTrials.gov identifier: NCT03084471) 12, in which patients who had progressed on chemotherapy received durvalumab (150 mg every 4 weeks until progression). Paired stool and blood samples for sMAdCAM-1 analysis were included in the pooled analysis.

The WELCOME (WEiL CORnell Medicine Employees) (protocol number IRB# 20-04021831) trial was conducted at Weill Cornell Medicine (WCM) and New York Presbyterian Hospital (NYP). The protocol is available at <https://research.weill.cornell.edu/NYPWelcomeStudy13>.

The Flemish study on Environment, Genes and Health Outcomes (FLEMENGHO) received ethical approval from the Ethics Committee of the University of Leuven (S67011). The FLEMENGHO cohort represents a random population sample stratified by sex and age from a geographically defined area in northern Belgium 14.

The reported clinical trials comply with all relevant ethical regulations on Research Involving Human Subjects.

Data collection

Clinical trials

JAVELIN Renal 101 is a multicenter, randomized, open-label, phase III clinical trial evaluating the efficacy and safety of avelumab plus axitinib versus sunitinib monotherapy in patients with previously untreated advanced RCC with a clear-cell component. A total of 886 adults were enrolled and randomized 1:1 to receive either avelumab (10 mg/kg IV every 2 weeks) plus axitinib (5 mg orally twice daily) or sunitinib (50 mg orally once daily for 4 weeks in a 6-week cycle). For alignment within the study, a single cycle consisted of 6 weeks for both treatment arms. The trial design has been previously described, and results are reported per CONSORT guidelines 1,2. The co-primary endpoints were progression-free survival (PFS) and overall survival (OS) in patients with PD-L1–positive tumors 1,3. A key secondary endpoint was PFS in the overall population; other endpoints included objective response rate (ORR). Efficacy data reported here reflect the second interim analysis of the JAVELIN Renal 101 trial, with a data cutoff of January 2019. Blood samples were collected at screening and on multiple days within cycles 1, 2, and 3, prior to treatment. Available baseline and cycle 3 samples were used in this analysis. Collection included whole blood in dipotassium ethylenediaminetetraacetic acid (K₂EDTA) and silica-coated tubes for plasma and serum separation, respectively. Sample availability varied based on patient consent, local regulations, sample pairing, volume constraints, and site-level data reporting. The protocol has been previously published 1.

GETUG-AFU 26 NIVOREN trial is a French, multicenter, prospective, phase II clinical trial evaluating the activity and safety of nivolumab in patients with metastatic ccRCC who had previously failed on or after an anti-angiogenic regimen, as previously published 4–6. Participants received nivolumab at 3 mg/kg every two weeks and underwent radiological assessment every 8–12 weeks. Treatment was continued until disease progression, unacceptable toxicity, withdrawal of consent, or death. The primary endpoint was to assess the incidence of high-grade adverse events (Grades 3–4 and Grade 5, as per CTCAE v4.0) 4. Secondary endpoints included ORR, PFS, OS, and exploration of candidate blood biomarkers associated with response and/or prognosis to treatment. Blood samples were collected before and on different visits after Nivolumab start. Available baseline, cycle 3, cycle 7 and progression visit samples were used in this analysis.

SURF trial is a French prospective, randomized, open-label phase IIb study that included patients with metastatic ccRCC treated with sunitinib at a standard 50 mg daily for 4 weeks, followed by a 2-weeks rest period (4/2) 7. Patients requiring a dose adjustment due to toxicity were randomized between the standard 4/2 schedule at a reduced dose of 37.5 mg daily and the experimental 2/1 schedule at 50 mg daily. The primary objective was to assess the median duration of sunitinib treatment in each group. Key secondary objectives included PFS, OS, time to randomization, ORR, safety, sunitinib dose intensity, health-related quality of life, and the description of main drivers triggering randomization. An exploratory endpoint included the identification of blood biomarkers related to the activity and/or toxicity of sunitinib. Available baseline blood samples were used in this report. The protocol has been previously published 8.

RCC ONCOBIOTICS is a multicentric study evaluating gut microbiota related biomarkers associated with outcome in advanced RCC treated with ICI alone or in combination with TKI at Gustave Roussy, in France. The study followed standard care until disease progression, unacceptable toxicity, or completion of 2 years of ICI treatment. Eligibility criteria and baseline data, including recent medications, are in the trial protocol and recorded in electronic case report forms. Blood and stool samples were collected before and on different visits after treatment start.

The ONCOBIOME network dataset 9,10 includes data from different cancer cohorts. Data from patients with lung cancer were obtained from the Lung ONCOBIOTICS study (ClinicalTrials.gov identifier: NCT04567446), a multicenter trial conducted across 14 centers in France and Canada. This study assessed the impact of the microbiome on treatment outcomes in patients with advanced non–small cell lung cancer (NSCLC) receiving anti–PD-(L)1 therapies, either alone or with chemotherapy. Patients were followed under standard care until disease progression, unacceptable toxicity, or completion of two years of ICI therapy. Eligibility criteria and baseline data, including recent medications, were recorded in trial protocols and electronic case report forms. Baseline stool and paired blood samples for sMAdCAM-1 analysis were included in the pooled analysis. Data from patients with colorectal cancer were from the AtezoTRIBE study (ClinicalTrials.gov identifier: NCT03721653) 11, a phase II trial enrolling 218 patients with unresectable stage IV colorectal cancer. Participants were randomized 2:1 to receive FOLFOXIRI plus bevacizumab with or without atezolizumab (anti–PD-L1). All patients were treatment-naïve at the time of initial stool collection. Paired baseline stool and blood samples for sMAdCAM-1 analysis were included in the pooled analysis. Data from patients with bladder cancer were sourced from the French cohort of the STRONG phase IIb trial (ClinicalTrials.gov identifier: NCT03084471) 12, in which patients who had progressed on chemotherapy received durvalumab (150 mg every 4 weeks until progression). Paired stool and blood samples for sMAdCAM-1 analysis were included in the pooled analysis.

The WELCOME (WEiL CORnell Medicine Employees) (protocol number IRB# 20-04021831) trial was conducted at Weill Cornell Medicine (WCM) and New York Presbyterian Hospital (NYP). The protocol is available at <https://research.weill.cornell.edu/NYPWelcomeStudy13>.

The Flemish study on Environment, Genes and Health Outcomes (FLEMENGHO) received ethical approval from the Ethics Committee of the University of Leuven (S67011). The FLEMENGHO cohort represents a random population sample stratified by sex and age from a geographically defined area in northern Belgium 14.

The reported clinical trials comply with all relevant ethical regulations on Research Involving Human Subjects.

Outcomes

In the current work, we asked whether sMAdCAM-1 levels could serve as a biomarker of an immunosuppressive microbiota linked to resistance to ICI and/or TKI regimens specifically in patients with metastatic RCC (mRCC). We investigated the distribution and biological significance of baseline and on-treatment sMAdCAM-1 levels in three independent cohorts of patients with mRCC: the JAVELIN Renal 101 trial (NCT02684006) the SURF trial (NCT02689167) and the GETUG-AFU26-NIVOREN trial (NCT0313335). Overall Survival (OS) was defined as the total length of time from the start of treatment until death from any cause (months). Progression-Free Survival (PFS) was defined as the time from the start of treatment until the cancer progresses or the patient dies from any cause, whichever comes first (months).

Plants

Seed stocks

NA

Novel plant genotypes

NA

Authentication

NA